

# Geometry of system-bath coupling and gauge fields in bosonic ladders: manipulating currents and driving phase transitions

Chu Guo<sup>1</sup> and Dario Poletti<sup>1</sup>

<sup>1</sup>*Singapore University of Technology and Design, 8 Somapah Road, 487372 Singapore*

Quantum systems in contact with an environment display a rich physics emerging from the interplay between dissipative and Hamiltonian terms. We consider a dissipative boundary driven ladder in presence of a gauge field which can be implemented with ion microtraps arrays. The dissipation stimulates currents while the gauge field tends to steer the flow. We show that depending on the geometry of coupling to the baths and of the strength of the gauge field, non-equilibrium phase transitions emerge strongly modifying the currents both in magnitude and spatial distribution.

Quantum systems in contact with an environment can present a very rich phenomenology due to the interplay between the Hamiltonian and dissipative dynamics. While the Hamiltonian can allow the emergence of quantum phase transitions, the dissipator can drive the system to a particular steady state (or more than one) the properties of which vary depending on the Hamiltonian itself. In these systems non-equilibrium phase transitions may occur [1–4]. Recent advances on quantum fluids of light [5], and on ultracold gases in cavities [6] have allowed experimental exploration of this physics.

A particularly important set of open systems is the boundary driven systems in which the set-up is connected at its boundaries to the environment. A typical example is that of a chain of particles connected, at its extremities, to two different baths, thus imposing a flow within the system. This scenario has been studied both theoretically and experimentally for various kinds of physical realizations including spin systems, photonic lattices, ions, metals, semiconductors and Josephson junctions arrays [7, 8]. Experiments with ion traps promise to be an ideal set-up to simulate boundary driven systems [9–11].

Abelian gauge fields, like the magnetic field acting on electrons, are known to be able to steer the motion of particles while they are transported. The quantum Hall effect is a striking example of the effects of a gauge field on transport [12, 13]. In recent experiments with Josephson junctions it has been possible to modify heat transport with a magnetic field [14]. Moreover, experimental advances have allowed the production of synthetic gauge fields with ultracold atoms [15, 16]. A theoretical proposal has described how to produce synthetic gauge fields in microtrap arrays for ions [17]. A simple geometry which can show the nontrivial effects of a gauge field is that of a ladder, i.e. two connected chains. This geometry has been extensively studied both in Josephson junctions arrays and bosonic atoms in optical lattices also in presence of interactions [2, 18–22, 24, 25]. Here we stress the emergence of a quantum phase transition for bosonic particles characterized by the order parameter chiral current which is defined as the difference of current between the upper and the lower chains.

We study the interplay between the dissipation which

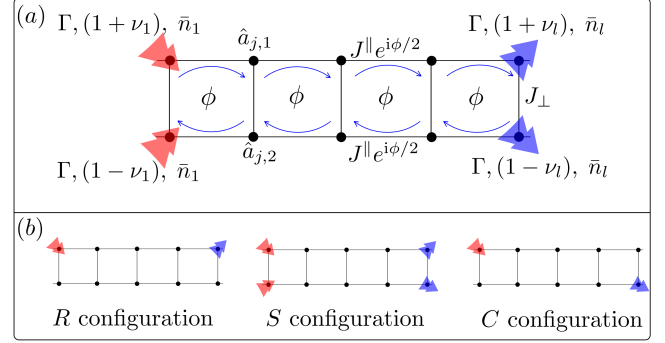


FIG. 1: (color online) (a) Ladder made of two coupled linear chains, referred to as legs of the ladder, with local bosonic excitations described by the annihilation operators at site  $j$   $\hat{a}_{j,p}$  where  $p = 1, 2$  respectively for the upper and the lower leg.  $J^{\perp}$  is the tunnelling between the legs, on what are referred to as rungs of the ladder, while  $J^{\parallel}$  is the amplitude of tunnelling between sites in the legs. A gauge field imposes a phase  $\phi$ . The coupling to the baths is represented by the thick arrows. Each bath is characterized by the average density of bosons  $\bar{n}_j$  the bath itself imposes on the rung  $j$  and the strength of the coupling  $\Gamma(1 \pm \nu_j)$ . (b) Three characteristic configurations: in the  $R$  (reflection symmetric) configuration the baths are coupled only to the upper chain, in the  $S$  (symmetric) configuration they are equally coupled to both chains while in the  $C$  (centrosymmetric) configuration one bath is coupled to upper chain while the other to the lower one. Note that the configurations are only symmetric regarding the geometric coupling to the bath but not considering the baths' parameters.

favours current flow in the system and the gauge potential which tends to steer it. The field can also cause significant changes in the energy levels' structure. We find that by tuning this field, combined with altering the geometry of the system-bath coupling, it is possible to drive non-equilibrium phase transitions which significantly affect the current flow. In particular, one phase transition affects the magnitude of the total current and occurs when a gap opens in the ladder's energy spectrum. This transition, depending on the geometry of the coupling, is also associated with an abrupt change of the chiral current. Within this set of geometries another non-equilibrium transition can occur for the chiral

currents related to the quantum phase transition. With symmetry considerations we can also show that the current is symmetric to a reversal of gauge field and also predict the presence of chiral currents.

The system we study is represented in Fig.1: a ladder made of two coupled chains (or legs) of  $l$  local bosonic modes which is coupled at its extremities to four baths. This could be realized with ion trap microarrays [17] which are driven at the boundaries by side-band cooling [26]. The evolution of an observable  $\hat{O}$  is given by

$$\frac{d\hat{O}}{dt} = -\frac{i}{\hbar} [\hat{O}, \hat{H}] + \mathcal{D}_H(\hat{O}) \quad (1)$$

where the Hamiltonian is given by  $\hat{H} = -\left(\sum_{j,p} J^{\parallel} e^{i(-1)^{p+1}\phi/2} \hat{a}_{j,p}^{\dagger} \hat{a}_{j+1,p} + J^{\perp} \sum_j \hat{a}_{j,1}^{\dagger} \hat{a}_{j,2}\right) + \text{H.c.}$  Here  $J^{\parallel}$  is the tunnelling constant in the legs,  $J^{\perp}$  for the rungs, while  $\hat{a}_{j,p}$  ( $\hat{a}_{j,p}^{\dagger}$ ) annihilates (creates) a boson in the upper (for  $p=1$ ) or lower ( $p=2$ ) chain at the  $j$ -th rung of the ladder. The tunnelling in the legs has a complex phase  $\phi/2$  due to our choice of the gauge. The coupling to the baths is modelled by a dissipator  $\mathcal{D}_H(\hat{O}) = \sum_{j,p} \tilde{\Gamma}_{j,p} \left[ \bar{n}_j \left( \hat{a}_{j,p} \hat{O} \hat{a}_{j,p}^{\dagger} - \hat{a}_{j,p}^{\dagger} \hat{O} \hat{a}_{j,p} \right) + (\bar{n}_j + 1) \left( \hat{a}_{j,p}^{\dagger} \hat{O} \hat{a}_{j,p} - \hat{a}_{j,p}^{\dagger} \hat{O} \hat{a}_{j,p} \right) + \text{H.c.} \right]$  in Lindblad form [27, 28] where  $j = 1$  or  $l$ ,  $\tilde{\Gamma}_{j,p} = \Gamma(1 - (-1)^p \nu_j)$  is the coupling constant of the bosons at site  $j$  and  $\bar{n}_j$  is the local particle density that the dissipator would impose to the ion if isolated.  $\Gamma$  is the overall coupling constant while  $\nu_j$  is the asymmetric component of the dissipative coupling to the baths. Varying the values of  $\nu_j$  make the coupling to the upper chain different from that to the lower, gradually turning the system from the  $S$  ( $\nu_j = 0$ ) to the  $R$  or  $C$  configurations depicted in Fig.1(b). As we shall see later in detail, changing  $\nu_j$  strongly affects the current flow generated in the ladder.

*Total current:* We study the current in the (unique) steady state of the system [29]. The total current,  $\mathcal{J} = \sum_p \mathcal{J}_{j,p}$ , is given by the sum of the current in the legs  $\mathcal{J}_{j,p}$ . The gauge invariant leg and rung particle currents are  $\mathcal{J}_{j,p} = \left\langle iJ^{\parallel} e^{i(-1)^{p+1}\phi/2} \hat{a}_{j,1}^{\dagger} \hat{a}_{j+1,1} + \text{H.c.} \right\rangle$  and  $\mathcal{J}_{j,1 \rightarrow 2} = \left\langle iJ^{\perp} \hat{a}_{j,1}^{\dagger} \hat{a}_{j,2} + \text{H.c.} \right\rangle$ , derived from the continuity equations  $\partial \langle \hat{n}_{j,1} \rangle / \partial t = \mathcal{J}_{j-1,1} - \mathcal{J}_{j,1} - \mathcal{J}_{j,1 \rightarrow 2}$  and  $\partial \langle \hat{n}_{j,2} \rangle / \partial t = \mathcal{J}_{j-1,2} - \mathcal{J}_{j,2} - \mathcal{J}_{j,2 \rightarrow 1}$  for  $1 < j < l$ .

Since the total current is independent on the rung number we drop the sub-index  $j$ . Symmetry considerations show that the current is symmetric under the transformation  $\phi \rightarrow -\phi$  (see [30] section I.C.1). The current in the system is ballistic (see [30] section VII) as it is approximately constant as the size of the system increases.

Tuning the phase  $\phi$  allows to vary the total current  $\mathcal{J}$  transported in the ladder. In particular, for sufficient coupling strength to the baths  $\Gamma$ , and asymmetric configuration, the current undergoes an abrupt change show-

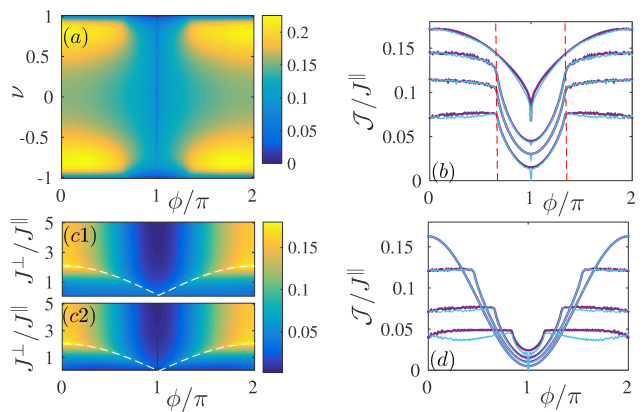


FIG. 2: (color online) (a) Total current in the ladder as a function of phase  $\phi$  and asymmetric coupling  $\nu$ . In the positive range of  $\nu$  we have chosen  $\nu_1 = \nu_l = \nu$  while in the negative range  $\nu_1 = -\nu_l = -\nu$ . This implies that the line  $\nu_l = 1$  corresponds to the  $R$  configuration,  $\nu_l = 0$  at the  $S$  configuration while  $\nu_l = -1$  is the  $C$  configuration. In (b) the light blue curves are for  $\nu_l > 0$  while the dark purple for  $\nu_l < 0$ . The values of  $\nu_l$  are, from top to bottom,  $\pm 0.4$ ,  $\pm 0.96$ ,  $\pm 0.98$  and  $\pm 1$ . The red vertical lines indicate the values of the phase  $\phi = 2\pi/3$  and  $4\pi/3$  at which, as discussed later, a gap opens between the lower and upper band in the energy spectrum of the ladder. (c) Depiction of the total current as a function of  $J^{\perp}$  and  $\phi$  for the  $R$  (c1) and  $C$  (c2) configurations. The white dashed lines are given by Eq.(3). (d) Selected curves from panels (c) showing  $\mathcal{J}$  versus  $\phi$  for  $J^{\perp}/J^{\parallel} = 0.5, 1, 1.5, 2.5$  (from bottom to top at  $\phi = 0$ ). The position of the transition shifts as  $J^{\perp}$  varies and it disappears for  $J^{\perp} \geq 2J^{\parallel}$ . The light blue and dark purple curves are for the  $C$  and  $R$  configurations respectively. In all the figures in this article the number of rungs  $l = 500$ ,  $\bar{n}_1 = 0.5$ ,  $\bar{n}_l = 0.1$  and the strength of the coupling to the baths is  $\Gamma = 5J^{\parallel}/\hbar$ .

ing a non-equilibrium quantum phase transition. This is clearly depicted in Fig.2: in panels (a-b) we show the current  $\mathcal{J}$  versus the phase  $\phi$  for different couplings to the baths, from the  $S$  ( $\nu = 0$ ), to the  $R$  ( $\nu = 1$ ) and  $C$  ( $\nu = -1$ ) configurations and intermediate cases. We stress two particular aspects: when the geometry of the coupling to the baths is close to the  $R$  or  $C$  configurations, the total current can be highly (or completely) suppressed around  $\phi = \pi$ . Moreover, there is a sharp change of the functional form of the current versus phase signalling the presence of a non-equilibrium phase transition (for a study of the dependence of the transition on the strength of the coupling  $\Gamma$  see [30] section VI). With Fig. 2(c,d) we explore the influence of the tunnelling between the legs  $J^{\perp}$ . Fig. 2(c,d) show the shift, and eventually the disappearance, of the transition as  $J^{\perp}$  is varied. The transition is demarked by the dashed white curve which is derived later to be Eq.(3).

*Chiral current:* An analysis of the chiral current  $\mathcal{J}_c = \sum_j (\mathcal{J}_{j,1} - \mathcal{J}_{j,2})/l$  shows that, unlike the unitary case without baths for which only one transition occurs, there

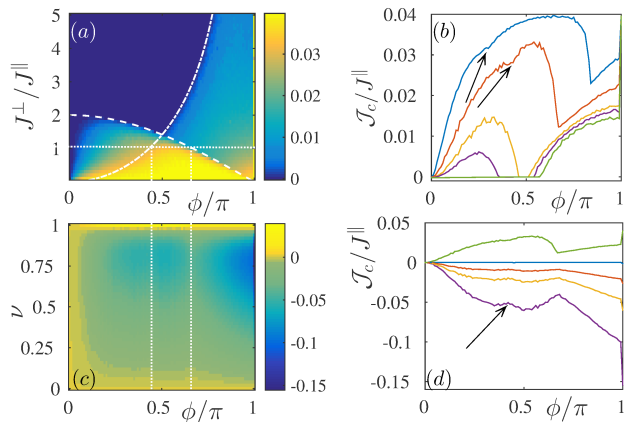


FIG. 3: (color online) (a) Chiral current as a function of perpendicular tunnelling  $J^\perp$  and phase  $\phi$ . (b) Chiral current versus  $\phi$  for the selected values of  $J^\perp/J^\parallel = 0.5, 1, 1.5, 1.7, 2$  (from top to bottom). In (a) we show that the two transitions happen at values of the phase given by Eq.(2), dash-dotted line, and (3), dashed line. (c) Chiral current, for  $J^\perp = J^\parallel$ , as function of  $\phi$  and  $\nu = \nu_1 = \nu_l$  which scans configurations between the  $S$  and  $R$ . The vertical lines highlight the positions of the two transitions which are given by the intersections of the  $J^\perp = J^\parallel$  curve with the curves give by Eqs.(2,3) in panel (a). (d) Chiral current versus phase  $\phi$  for  $\nu = \nu_1 = \nu_l = 0.02, 0.18, 0.38, 0.78, 1$  (from bottom to top) showing chiral current inversion. The arrows in (b) and (d) highlight one of the transitions.

can be two transitions. Moreover, symmetry guarantees that the chiral current vanishes for the symmetric coupling to the baths  $S$  and the centrosymmetric coupling  $C$  and scenarios in between ([30] section II). Results for the  $R$  configuration are depicted in Fig.3(a,b) where we show the combined effect of  $J^\perp$  and  $\phi$ . At a smaller value of  $J^\perp$ , the chiral current presents two abrupt changes in its derivative with respect to  $\phi$ , [these points are highlighted with arrows in top lines of Fig.3(b)], then, at intermediate values of  $J^\perp$  two regions with chiral current are clearly separated and drift apart until, at large values of  $J^\perp$ , the chiral current is only present at  $\phi = \pi$ . The transition becomes sharper as the size of the system is increased ([30] section V). In Fig.3(c,d) we study the role of the amplitude of the asymmetric coupling  $\nu$  as the system varies from the  $S$  towards the  $R$  configurations while keeping  $J^\perp = J^\parallel$ . The two transitions are highlighted by the white dotted lines in Fig. 3(c). We also note a chiral current inversion for large enough  $\nu$ , which is clearly shown in Fig.3(d) which depicts some horizontal cuts of Fig.3(c). The physical origin of this is different from [25].

*Bulk spectrum:* These transitions can be understood by studying the energy spectrum of an infinitely long ladder system which we will refer to as ‘bulk’. This is given by  $E_k^\pm = -2J^\parallel \cos(\phi/2) \cos(k) \pm$

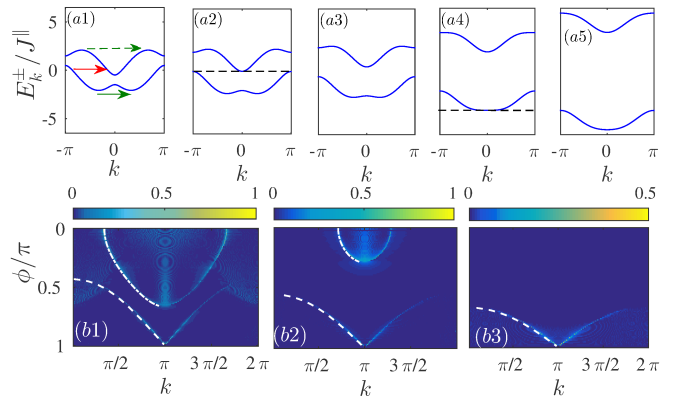


FIG. 4: (color online) (a1-5) Energy spectrum of the ladder for phase  $\phi = 2\pi/3$  and the amplitude of tunnelling in the bulk respectively  $J^\perp/J^\parallel = 0.5, 1, 1.5, 3, 5$ . The dashed line in (a2) highlights that this corresponds to the critical value of  $J^\perp$  at which the gap between the lower and upper band is 0. The dashed line in (a4) points out that  $J^\perp = 3J^\parallel$  is the critical value at which the minima have merged. (b1-b3) Momentum probability distribution for the current in the lower leg as a function of  $\phi$  and the momentum  $k$  for the  $R$  configuration (other configurations, except the symmetric  $S$  configuration present a similar structure). In the three plots  $J^\perp/J^\parallel$  is respectively 1, 1.8 and 3. The white dot-dashed lines are analytically obtained from Eq.(4) and highlight current due to bath induced intra-band coupling as, for example as depicted in (a1) by the green arrows. The white continuous lines is given by Eq.(5) and is due to inter-bands coupling [one example is the red arrow in (a1)]. Note that the point  $k = 0$  has been removed to make the patterns more visible.

$\sqrt{J^\perp{}^2 + [2J^\parallel \sin(\phi/2) \sin(k)]^2}$  where  $k$  is the quasi-momentum (see [30] section III for more details; the simpler cases of  $\phi = 0, \pi$  are treated in section IV). A depiction of five types of energy spectra for  $\phi = 2\pi/3$  for different values of  $J^\perp$  is given in Fig. 4(a1-a5). For smaller values of  $J^\perp$  the lower band features two minima and there exists a region of energies in which both the lower and higher bands are present [see Fig. 4(a1) for  $J^\perp = J^\parallel/2$ ]. For  $J^\perp = J^\parallel$ , Fig.4(a2), the system undergoes a phase transition as the two bands only have common values of the energy at  $\varepsilon = 0$  and will not have common values for larger values of  $J^\perp$ , Fig. 4(a3-5). The next transition occurs at  $J^\perp = 3J^\parallel$ , Fig. 4(a4), at which the two minima of the lower band converge and only one minimum is present for larger values of  $J^\perp$  [Fig.4(a5)]. The transition between one to two minima in the lower band is known to cause a quantum phase transition, in the Hamiltonian case, signalled by a change in the chiral current. The critical values of rung tunnelling  $\tilde{J}_\perp$  and critical phase  $\tilde{\phi}$  at which this quantum phase transition occurs can be readily computed by the spectrum giving

$$\tilde{J}_\perp = 2J^\parallel \tan(\tilde{\phi}/2) \sin(\tilde{\phi}/2). \quad (2)$$

This curve is depicted with a white dash-dotted line in

Fig.3(a) and clearly demarcates one of the two regions with chiral currents. This implies that the quantum phase transition in the bulk ladder system induces chiral currents also in the boundary driven system. However, this transition does not affect the total current  $\mathcal{J}$  to the same extent. The transition shown in Fig.2 occurs at different values of  $\phi$  and  $J^\perp$  and it is due to the opening of a gap between the lower and higher bands, Fig.4(a2), for

$$\bar{J}_\perp = 2J^\parallel \cos(\bar{\phi}/2). \quad (3)$$

This relation is depicted by the white dashed line in Figs.2(c1,c2) and 3(a) and separates at the same time the second region with chiral current and the region in which the total current is suppressed.

*Momentum space:* The presence of chiral currents and/or of current modulations can also be monitored by studying the momentum distribution of the current. As the total current  $\mathcal{J}$  is constant within the chain, we study the Fourier transform of the current in the lower leg  $\mathcal{J}_{j,2}$  which we denote by  $\mathcal{J}^{k,2}$ . In Fig.4(b1-b3) we show  $|\mathcal{J}^{k,2}|$  for a ladder coupled to the baths in the  $R$  configuration of length  $l = 500$  with  $J^\perp$  respectively given by  $J^\parallel$ ,  $1.8J^\parallel$ , and  $3J^\parallel$ . Comparing Fig.4(b1-b3) with Fig.3(a) we notice that modulations of the current in the legs is concurrent with the presence of chiral currents. This is completely different from the Hamiltonian case in which, in the presence of chiral currents, there is no current in the rungs and hence no modulation of the current in the legs. Hence this is an effect purely due to the interplay between the Hamiltonian and the dissipative dynamics and, while the observable showing the transition is the same, its physical interpretation is different.

The modulations of the current are due to coupling between different momenta induced by the dissipator  $\mathcal{D}_H$  which couples more strongly quasi-momenta at the same energy. To show this we have overlain in Fig.4(b1-b3) [for clarity only for  $k \in (0, \pi)$ ] a white dot-dashed curve which is given by the value of the distance between the two minima (maxima) of the lower (higher) band,

$$\Delta k_{\text{intra},1} = -\Delta k_{\text{intra},2} = 2\arccos(\theta_{\text{intra}}) \quad (4)$$

where  $\theta_{\text{intra}} = \cot(\phi/2) \sqrt{\sin^2(\phi/2) + [J^\perp/(2J^\parallel)]^2}$ , derived in section III.A of [30]. The curve matches perfectly the peak in the momentum distribution. This shows that these peaks are due to dissipation induced intra-band coupling. In Fig. 4(b1-b3) we overlay the other peaks in  $|\mathcal{J}_{k,2}|$  by a white dashed line whose functional form is given by the analytical expression

$$\Delta k_{\text{inter},1} = -\Delta k_{\text{inter},2} = \pm\arccos(\theta_{\text{inter}}) \quad (5)$$

where  $\theta_{\text{inter}} = 2 \cos\left(\frac{\phi}{2}\right) [\cos(\phi/2) - (J^\perp/(2J^\parallel))]$  - 1. This is derived by computing the distance in  $k$ -space between the lower and higher bands, for  $k$  and  $k'$  with the

same energy  $E_k^+ = E_{k'}^-$ , as shown in [30], section III.B. Hence these modulations are due to inter-band coupling. This also explains why such modulations of the current are not present for  $J^\perp \geq 2J^\parallel$ , as for example in Fig.4(b3), for which a band gap exists for any value of  $\phi$ .

*Conclusions:* We have shown that the interplay between (1) the current-imposing baths at the boundaries, (2) their geometrical coupling to the ladder and (3) a gauge field which tends to alter the current flow and causes significant changes in the energy spectrum in the bulk system, result in non-equilibrium phase transitions in which the magnitude and the pattern of the current transported can change significantly. This phenomenology extends significantly the one studied in the ground-state of the Hamiltonian system. In particular we show the presence of two regions in which chiral currents are present and we connect the boundaries of these regions with (i) the emergence of two minima in the energy spectrum and (ii) an opening of a gap between the lower and higher bands. The opening of the gap also causes a significant reduction of the total current transferred. It should be stressed further the importance of the geometry of the coupling. Only for asymmetric geometries, like  $R$  and  $C$ , such phenomenology emerges while in the symmetric  $S$  configuration the rung current is always 0 and the non-equilibrium phase transitions do not occur (see [30] section II.E). Again for symmetry reasons, see section II.C in [30], the special point  $\phi = \pi$  can present  $l - 1$  dark modes, that is modes which are unaffected by the dissipation, in the  $R$  configuration while the current can be exactly equal to 0 in the  $C$  configuration ([30] section II.A), as shown in Fig.2(b,d).

*Acknowledgements:* We acknowledge insightful discussions with U. Bissbort, R. Fazio, B. Grémaud, C. Kollath, M. Mukherjee and S. Yang. D.P. acknowledges support from AcRF MOE Tier-II (project MOE2014-T2-2-119, WBS R-144-000-350-112) and AcRF MOE Tier-I (project SUTDT12015005).

- 
- [1] S. Diehl, A. Micheli, A. Kantian, B. Kraus, H.P. Büchler, P. Zoller, Nat. Phys. **4**, 878 (2008).
  - [2] S. Diehl, A. Tomadin, A. Micheli, R. Fazio, P. Zoller, Phys. Rev. Lett. **105**, 015702 (2010).
  - [3] E.G. Dalla Torre, E. Demler, T. Giamarchi, E. Altman, Nat. Phys. **6**, 806 (2010).
  - [4] M. Ludwig, F. Marquardt, Phys. Rev. Lett. **111**, 073603 (2013).
  - [5] I. Carusotto, C. Ciuti, Rev. Mod. Phys. **85**, 299 (2013).
  - [6] K. Baumann, C. Guerlin, F. Brennecke, T. Esslinger, Nature **464**, 1301 (2010).
  - [7] M. Michel, J. Gemmer, and G. Mahler, Int. J. Mod. Phys. B **20**, 4855 (2006).
  - [8] G. Benenti, G. Casati, C. Mejia-Monasterio, M. Peyrard, arXiv:1512.06889 (2015).
  - [9] A. Bermudez, M. Bruderer, M.B. Plenio, Phys. Rev. Lett.

- 111**, 040601 (2013).
- [10] M. Ramm, T. Pruttivarasin, H. Häffner, *New J. Phys.* **16** 063062, (2014).
- [11] C. Guo, M. Mukherjee, D. Poletti, *Phys. Rev. A.* **92**, 023637 (2015).
- [12] K. v. Klitzing, G. Dorda, and M. Pepper, *Phys. Rev. Lett.* **45**, 494 (1980).
- [13] R. B. Laughlin, *Phys. Rev. B* **23**, 5632(R) (1981).
- [14] F. Giazotto, *Nat. Phys.* **11**, 527 (2015).
- [15] J. Dalibard, F. Gerbier, G. Juzeliunas, P. Ohberg, *Rev. Mod. Phys.* **83**, 1523 (2011).
- [16] N. Goldman, G. Juzeliunas, P. Ohberg, I. B. Spielman, *Rep. Prog. Phys.* **77**, 126401 (2014).
- [17] A. Bermudez, T. Schaetz, D. Porras, *Phys. Rev. Lett.* **107**, 150501 (2011).
- [18] M. Kardar, *Phys. Rev. B* **33**, 3125 (1986).
- [19] E. Granato, *Phys. Rev. B* **42**, 4797(R) (1990).
- [20] C. Denniston, C. Tang, *Phys. Rev. Lett.* **75**, 3930 (1995).
- [21] E. Orignac, T. Giamarchi, *Phys. Rev. B* **64**, 144515 (2001).
- [22] M. Atala, M. Aidelsburger, M. Lohse, J. T. Barreiro, B. Paredes, I. Bloch, *Nat. Phys.* **10**, 588 (2014).
- [23] A. Tokuno, A. Georges, *New J. Phys.* **16**, 073005 (2014).
- [24] M. Piraud, F. Heidrich-Meisner, I. P. McCulloch, S. Greschner, T. Vekua, U. Schollwöck, *Phys. Rev. B* **91**, 140406(R), (2015).
- [25] S. Greschner, M. Piraud, F. Heidrich-Meisner, I. P. McCulloch, U. Schollwöck, T. Vekua, *Phys. Rev. Lett.* **115**, 190402 (2015).
- [26] D. Leibfried, R. Blatt, C. Monroe, D. Wineland, *Rev. Mod. Phys.* **75**, 281 (2003).
- [27] G. Lindblad, *Comm. Math. Phys.* **48**, 119 (1976).
- [28] V. Gorini, A. Kosakowski, E.C.G. Sudarshan, *J. Math. Phys.* **17**, 821 (1976).
- [29] Except for the case  $\phi = \pi$  in the  $R$  configuration and also  $l$  even for which there exist  $l - 1$  dark states which are not affected by the dissipation [30].
- [30] see Supplementary Material.
-

## Supplementary material

### I. The Liouvillian superoperator

The Hamiltonian for the bosonic ladder system for a single band can be given by

$$\begin{aligned} \hat{H} = & - \sum_{p=1,2} \sum_{j=1}^{l-1} [J_{j,p}^{\parallel} e^{iA_{j,p}^{\parallel}} \hat{a}_{j,p}^{\dagger} \hat{a}_{j+1,p} + \text{H.c.}] - \sum_{j=1}^l [J_j^{\perp} e^{iA_j^{\perp}} \hat{a}_{j,1}^{\dagger} \hat{a}_{j,2} + \text{H.c.}] \\ & + \sum_{j=1}^l \sum_{p=1,2} \mu_{j,p} \hat{n}_{j,p} \end{aligned} \quad (\text{S.1})$$

where the parameters here considered are described in the main paper. We consider the local dissipation  $\mathcal{D}$  is given by

$$\mathcal{D}(\hat{\rho}) = \sum_j \sum_p \Lambda_{j,p}^+ (\hat{a}_{j,p}^{\dagger} \hat{\rho} \hat{a}_{j,p} + \hat{a}_{j,p} \hat{a}_{j,p}^{\dagger} \hat{\rho}) + \Lambda_{j,p}^- (\hat{a}_{j,p} \hat{\rho} \hat{a}_{j,p}^{\dagger} - \hat{a}_{j,p}^{\dagger} \hat{a}_{j,p} \hat{\rho}) + \text{H.c.} \quad (\text{S.2})$$

In the following we show that we can diagonalize a special kind of open system and find the normal modes, using an approach similar to the Bogoliubov transformation. In various aspects this derivation resembles [1]. Since the proof is independent of the dimension of the system, we will just use operators with a single index, such as  $\hat{a}_i$  and  $\hat{a}_i^{\dagger}$ , to denote the creation and annihilation operators. For systems with dimensions larger than one, simply a one to one map to transfer the single index to multi-indices is needed. For instance, in the bosonic ladder with  $l$  rungs, the single index  $2i - 1$  will be mapped to  $(i, 1)$ , and  $2i$  will be mapped to  $(i, 2)$ .

In the following we consider a general open system with Hamiltonian  $\hat{H} = \sum_{i,j=1}^L h_{ij} a_i^{\dagger} a_j$ , and  $\mathcal{D}(\rho) = \sum_{i,j=1}^L (\Lambda_{i,j}^+ (a_i^{\dagger} \rho a_j - a_j a_i^{\dagger} \rho) + \Lambda_{i,j}^- (a_i \rho a_j^{\dagger} - a_j^{\dagger} a_i \rho) + \text{H.c.})$ , where  $L$  is the total number of possible indices.  $h$ ,  $\Lambda^+$  and  $\Lambda^-$  are hermitian matrices. Note that we have dropped the hat from  $\hat{\rho}$  and the creation and annihilation operators to simplify the notation. We denote the  $L \times L$  matrix  $\bar{h}$  as

$$\bar{h} = \frac{1}{2} \left( -ih - \Lambda^+ - \Lambda^{-t} \right); \quad (\text{S.3})$$

Note that with  $^t$  we indicate the transpose of the matrix. We now perform a mapping from density matrices with elements corresponding to  $|i\rangle\langle j|$ , This results in mapping  $a_i$  acting on the left of the density matrix to  $a_n$  (acting to the left of the vector) with  $n = i$  while  $a_i$  acting to the right of the density matrix is mapped to  $\hat{a}_n^{\dagger}$  (naturally also acting to the left of the vector) with  $n = L + i$ . This allows to write the Liouvillian super operator  $\mathcal{L}$ , defined from  $\mathcal{L}(\hat{\rho}) = -i/\hbar [\hat{H}, \rho] + \mathcal{D}(\rho)$ , in the following left and right basis

$$\begin{pmatrix} \mathbf{a}_{1 \rightarrow L}^{\dagger} \\ \mathbf{a}_{(L+1) \rightarrow 2L}^{(L+1) \rightarrow 2L} \\ \mathbf{a}_{1 \rightarrow L} \\ \mathbf{a}_{(L+1) \rightarrow 2L}^{\dagger} \end{pmatrix}, \left( \mathbf{a}_{1 \rightarrow L} \quad \mathbf{a}_{(L+1) \rightarrow 2L}^{\dagger} \quad \mathbf{a}_{1 \rightarrow L}^{\dagger} \quad \mathbf{a}_{(L+1) \rightarrow 2L} \right), \quad (\text{S.4})$$

where  $\mathbf{a}_{1 \rightarrow L}$  means  $\{\hat{a}_1, \hat{a}_2, \dots, \hat{a}_L\}$ , and the coefficients forming  $\mathcal{L}$  become the matrix

$$\begin{pmatrix} \bar{h} & \Lambda^+ & \mathbf{0} & \mathbf{0} \\ \Lambda^{-t} & \bar{h}^{\dagger} & \mathbf{0} & \mathbf{0} \\ \mathbf{0} & \mathbf{0} & \bar{h}^t & \Lambda^- \\ \mathbf{0} & \mathbf{0} & \Lambda^{+t} & \bar{h}^{\dagger t} \end{pmatrix}. \quad (\text{S.5})$$

which is block diagonal. This means that one only needs to consider the small matrix

$$M = \begin{pmatrix} \bar{h} & \Lambda^+ \\ \Lambda^{-t} & \bar{h}^{\dagger} \end{pmatrix} \quad (\text{S.6})$$

and its transpose. Hence  $\mathcal{L}$  can be written in the following compact form

$$\mathcal{L} = \begin{pmatrix} \mathbf{a}_{1 \rightarrow L}^{\dagger} & \mathbf{a}_{L+1 \rightarrow 2L} \end{pmatrix} M \begin{pmatrix} \mathbf{a}_{1 \rightarrow L} \\ \mathbf{a}_{L+1 \rightarrow 2L}^{\dagger} \end{pmatrix} + \begin{pmatrix} \mathbf{a}_{1 \rightarrow L} & \mathbf{a}_{L+1 \rightarrow 2L}^{\dagger} \end{pmatrix} M^t \begin{pmatrix} \mathbf{a}_{1 \rightarrow L}^{\dagger} \\ \mathbf{a}_{L+1 \rightarrow 2L} \end{pmatrix} + \text{tr}(\Lambda^- - \Lambda^+). \quad (\text{S.7})$$

### I.A. Solving for the steady state

In general  $M$  is not an hermitian matrix and it cannot always be diagonalized, however in the following we start from the assumption that we know a transformation which can diagonalize  $M$  and preserves bosonic commutation relations

$$\begin{pmatrix} \mathbf{a}_{1 \rightarrow L} \\ \mathbf{a}_{L+1 \rightarrow 2L}^\dagger \end{pmatrix} = W_1 \begin{pmatrix} \mathbf{b}_{1 \rightarrow L} \\ \mathbf{b}'_{L+1 \rightarrow 2L} \end{pmatrix}, \begin{pmatrix} \mathbf{a}_{1 \rightarrow L}^\dagger \\ \mathbf{a}_{L+1 \rightarrow 2L} \end{pmatrix} = W_2 \begin{pmatrix} \mathbf{b}'_{1 \rightarrow L} \\ \mathbf{b}_{L+1 \rightarrow 2L} \end{pmatrix}. \quad (\text{S.8})$$

This assumption is a posteriori verified in most of the cases we consider. Using this transformation we get

$$\mathcal{L} = (\mathbf{b}'_{1 \rightarrow L} \ \mathbf{b}_{L+1 \rightarrow 2L}) W_2^t M W_1 \begin{pmatrix} \mathbf{b}_{1 \rightarrow L} \\ \mathbf{b}'_{L+1 \rightarrow 2L} \end{pmatrix} + (\mathbf{b}_{1 \rightarrow L} \ \mathbf{b}'_{L+1 \rightarrow 2L}) W_1^t M^t W_2 \begin{pmatrix} \mathbf{b}'_{1 \rightarrow L} \\ \mathbf{b}_{L+1 \rightarrow 2L} \end{pmatrix} + \text{tr}(\Lambda^- - \Lambda^+). \quad (\text{S.9})$$

Since  $\left[ \begin{pmatrix} \mathbf{a}_{1 \rightarrow L} \\ \mathbf{a}_{L+1 \rightarrow 2L}^\dagger \end{pmatrix}, \begin{pmatrix} \mathbf{a}_{1 \rightarrow L}^\dagger \\ \mathbf{a}_{L+1 \rightarrow 2L} \end{pmatrix}^t \right] = \Sigma_L$ , and requiring  $\left[ \begin{pmatrix} \mathbf{b}_{1 \rightarrow L} \\ \mathbf{b}'_{L+1 \rightarrow 2L} \end{pmatrix}, \begin{pmatrix} \mathbf{b}'_{1 \rightarrow L} \\ \mathbf{b}_{L+1 \rightarrow 2L} \end{pmatrix}^t \right] = \mathbf{1}_{2L}$ . We get

$$\Sigma_L = W_1 \Sigma_L W_2^t \iff W_2 = \Sigma_L W_1^{t-1} \Sigma_L \quad (\text{S.10})$$

Here we have used the notation  $\mathbf{1}_l$  for an identity matrix of size  $l$ . Other useful notations are

$$\Sigma_L = \begin{pmatrix} \mathbf{1}_L & 0 \\ 0 & -\mathbf{1}_L \end{pmatrix}, \Upsilon_L = \begin{pmatrix} 0 & \mathbf{1}_L \\ \mathbf{1}_L & 0 \end{pmatrix}, \Omega_L = \begin{pmatrix} 0 & \mathbf{1}_L \\ -\mathbf{1}_L & 0 \end{pmatrix}, \quad (\text{S.11})$$

where these matrices satisfy the relations

$$\Sigma_L^2 = \mathbf{1}_{2L}, \Upsilon_L^2 = \mathbf{1}_{2L}, -\Omega_L^2 = \mathbf{1}_{2L}, \Sigma_L \Upsilon_L = -\Upsilon_L \Sigma_L = \Omega_L. \quad (\text{S.12})$$

It follows that

$$\begin{aligned} \mathcal{L} &= (\mathbf{b}'_{1 \rightarrow L} \ \mathbf{b}_{L+1 \rightarrow 2L}) \Sigma_L W_1^{-1} \Sigma_L M W_1 \begin{pmatrix} \mathbf{b}_{1 \rightarrow L} \\ \mathbf{b}'_{L+1 \rightarrow 2L} \end{pmatrix} \\ &+ (\mathbf{b}_{1 \rightarrow L} \ \mathbf{b}'_{L+1 \rightarrow 2L}) W_1^t M^t \Sigma_L W_1^{t-1} \Sigma_L \begin{pmatrix} \mathbf{b}'_{1 \rightarrow L} \\ \mathbf{b}_{L+1 \rightarrow 2L} \end{pmatrix} + \text{tr}(\Lambda^- - \Lambda^+) \\ &= (\mathbf{b}'_{1 \rightarrow L} \ \mathbf{b}_{L+1 \rightarrow 2L}) \Sigma_L (W_1^{-1} \Sigma_L M W_1) \begin{pmatrix} \mathbf{b}_{1 \rightarrow L} \\ \mathbf{b}'_{L+1 \rightarrow 2L} \end{pmatrix} \\ &+ (\mathbf{b}_{1 \rightarrow L} \ \mathbf{b}'_{L+1 \rightarrow 2L}) (W_1^{-1} \Sigma_L M W_1)^t \Sigma_L \begin{pmatrix} \mathbf{b}'_{1 \rightarrow L} \\ \mathbf{b}_{L+1 \rightarrow 2L} \end{pmatrix} + \text{tr}(\Lambda^- - \Lambda^+) \end{aligned} \quad (\text{S.13})$$

We find that the problem reduces to diagonalize  $\Sigma_L M$ , if such  $W_1$  can be found, that is,

$$W_1^{-1} (\Sigma_L M) W_1 = \text{diag}(\beta_1, \beta_2, \dots, \beta_{2L}), \quad (\text{S.14})$$

where  $\text{diag}(\vec{v})$  is a diagonal matrix with the elements of  $\vec{v}$  on its diagonal. Hence we get the following compact form for  $\mathcal{L}$  :

$$\mathcal{L} = 2 \sum_{i=1}^L (\beta_i b'_i b_i - \beta_{L+i} b'_{L+i} b_{L+i}) + \sum_{i=1}^L (\beta_i - \beta_{L+i}) + \text{tr}(\Lambda^- - \Lambda^+). \quad (\text{S.15})$$

Noticing the relation

$$\Upsilon M \Upsilon = M^\dagger; \quad (\text{S.16})$$

we find that if  $x = \begin{pmatrix} \mathbf{u} \\ \mathbf{v} \end{pmatrix}$  is a right eigenvector of  $\Sigma_L M$  to  $\omega$ , then  $x^\dagger \Omega$  is a left eigenvector of  $\Sigma_L M$  to  $-\omega^*$ . In fact

$$\begin{aligned} \Sigma_L M x = \omega x &\rightarrow x^\dagger M^\dagger \Sigma_L = \omega^* x^\dagger \\ &\rightarrow x^\dagger \Upsilon_L \Upsilon_L M^\dagger \Upsilon_L = \omega^* x^\dagger \Sigma_L \Upsilon_L \\ &\rightarrow x^\dagger \Upsilon_L M = \omega^* x^\dagger \Sigma_L \Upsilon_L. \end{aligned} \quad (\text{S.17})$$

This implies  $x^\dagger \Upsilon_L \Sigma_L \Sigma_L M = x^\dagger \Upsilon_L M = \omega^* x^\dagger \Sigma_L \Upsilon_L$ , which means  $x^\dagger \Omega_L \Sigma_L M = -\omega^* x^\dagger \Omega_L$ . Thus it follows that  $x^\dagger \Omega_L$  is a left eigenvector of  $\Sigma_L M$  to  $-\omega^*$ .

Moreover if  $x_1$  is a right eigenvector of  $\Sigma_L M$  to  $\omega_1$ , and  $x_2$  is a right eigenvector of  $\Sigma_L M$  to  $\omega_2$ , then if  $\omega_1 + \omega_2^* \neq 0$  then  $x_1^\dagger \Omega_L x_2 = 0$ . In fact

$$\Sigma_L M x_1 = \omega_1 x_1; \quad (\text{S.18})$$

$$\Sigma_L M x_2 = \omega_2 x_2, \quad (\text{S.19})$$

then

$$x_1^\dagger \Omega_L \Sigma_L M = -\omega_1^* x_1^\dagger \Omega_L; \quad (\text{S.20})$$

$$\Sigma_L M x_2 = \omega_2 x_2;$$

$$\rightarrow (\omega_1^* + \omega_2) x_1^\dagger \Omega_L x_2 = 0.$$

Since the right eigenvalues of  $\Sigma_L M$  always appear in pairs, we could list the eigenvalues and the corresponding eigenvectors of  $\Sigma_L M$  as  $W_1 = \omega_1, \omega_2, \dots, \omega_L, -\omega_1^*, \dots, \omega_L^*$ , with the right eigenvectors  $(\vec{x}_1, \vec{x}_2, \dots, \vec{x}_{2L})$ . Following the above arguments, we know that the left eigenvectors are  $(\vec{x}_{L+1}^\dagger; \vec{x}_{L+2}^\dagger; \dots; \vec{x}_{2L}^\dagger; \vec{x}_1^\dagger; \dots; \vec{x}_L^\dagger) \Omega_L = \Upsilon_L (\vec{x}_1^\dagger; \vec{x}_2^\dagger; \dots; \vec{x}_{2L}^\dagger) \Omega_L = \Upsilon_L W_1^\dagger \Omega_L$ .

We can choose to renormalize the right eigenvectors as

$$\Upsilon_L W_1^\dagger \Omega_L W_1 = \Sigma_L \Leftrightarrow \Omega_L W_1^\dagger \Omega_L W_1 = \mathbf{1}_{2L} \quad (\text{S.21})$$

so that we have

$$W_1^{-1} = \Omega_L W_1^\dagger \Omega_L, \quad (\text{S.22})$$

$$W_2 = -\Upsilon_L W_1^* \Upsilon_L. \quad (\text{S.23})$$

We can now define a new  $L \times L$  matrix  $P = \bar{h} + \Lambda^+ = (-ih + \Lambda^+ - \Lambda^{-t})/2$  for which we assume matrix  $P$  has the eigendecomposition  $PW_P = W_P \lambda_P$ , where  $W_P$  and  $\lambda_P$  are eigenvectors and eigenvalues. Then we find that  $(W_P; W_P)$  are  $L$  right eigenvectors (of length  $2L$ ) of  $\Sigma_L M$ , corresponding to  $\lambda_P$ , and  $(W_P^\dagger, -W_P^\dagger)$  are  $L$  left eigenvectors of  $\Sigma_L M$ , corresponding to  $-\lambda_P^*$ . This is derived using

$$\Sigma_L M (W_P; W_P) = (PW_P; PW_P) = (W_P; W_P) \lambda_P \quad (\text{S.24})$$

$$(W_P^\dagger, -W_P^\dagger) \Sigma_L M = (-W_P^\dagger P^\dagger, W_P^\dagger P^\dagger) = -\lambda_P^* (W_P^\dagger, -W_P^\dagger). \quad (\text{S.25})$$

Hence by denoting the remaining  $L$  right eigenvectors of  $\Sigma_L M$  as  $(C; D)$ , where  $C, D$  are  $L \times L$  matrix, we know that they are the right eigenvectors with eigenvalues  $-\lambda_P^*$ , which are paired with the left eigenvectors  $(W_P^\dagger, -W_P^\dagger)$ . Also  $(-D^\dagger, C^\dagger)$  will be the left eigenvectors corresponding the eigenvalues  $\lambda_P$ , which are paired with the right eigenvectors  $(W_P; W_P)$ . Therefore  $W_1$  and  $W_2$  can be written more explicitly as

$$W_1 = \begin{pmatrix} W_P & C \\ W_P & D \end{pmatrix}, \quad W_1^{-1} = \begin{pmatrix} -D^\dagger & C^\dagger \\ W_P^\dagger & -W_P^\dagger \end{pmatrix}, \quad (\text{S.26})$$

$$W_2 = -\begin{pmatrix} D^* & W_P^* \\ C^* & W_P^* \end{pmatrix}, \quad W_2^{-1} = \begin{pmatrix} W_P^t & -W_P^t \\ -C^t & D^t \end{pmatrix} \quad (\text{S.27})$$

which means

$$\mathbf{a}_{1 \rightarrow L} = W_P \mathbf{b}_{1 \rightarrow L} + C \mathbf{b}'_{L+1 \rightarrow 2L}; \quad (\text{S.28a})$$

$$\mathbf{a}_{L+1 \rightarrow 2L}^\dagger = W_P \mathbf{b}_{1 \rightarrow L} + D \mathbf{b}'_{L+1 \rightarrow 2L}; \quad (\text{S.28b})$$

$$\mathbf{a}_{1 \rightarrow L}^\dagger = -D^* \mathbf{b}'_{1 \rightarrow L} - W_P^* \mathbf{b}_{L+1 \rightarrow 2L}; \quad (\text{S.28c})$$

$$\mathbf{a}_{L+1 \rightarrow 2L} = -C^* \mathbf{b}'_{1 \rightarrow L} - W_P^* \mathbf{b}_{L+1 \rightarrow 2L}. \quad (\text{S.28d})$$

and the inverse equation

$$\mathbf{b}_{1 \rightarrow L} = W_P^\dagger \mathbf{a}_{1 \rightarrow L} + C^\dagger \mathbf{a}'_{L+1 \rightarrow 2L}; \quad (\text{S.29a})$$

$$\mathbf{b}'_{L+1 \rightarrow 2L} = W_P^\dagger \mathbf{a}_{1 \rightarrow L} - W_P^\dagger \mathbf{a}'_{L+1 \rightarrow 2L}; \quad (\text{S.29b})$$

$$\mathbf{b}'_{1 \rightarrow L} = W_P^t \mathbf{a}'_{1 \rightarrow L} - W_P^t \mathbf{a}_{L+1 \rightarrow 2L}; \quad (\text{S.29c})$$

$$\mathbf{b}_{L+1 \rightarrow 2L} = -C^t \mathbf{a}'_{1 \rightarrow L} + D^t \mathbf{a}_{L+1 \rightarrow 2L}. \quad (\text{S.29d})$$

Noticing that  $\sum \lambda_P = \text{tr}(P) = (-i \text{tr}(h) + \text{tr}(\Lambda^+) - \text{tr}(\Lambda^{-t}))/2$  and since  $(\lambda_P, -\lambda_P^*)$  corresponds to eigenvalues of  $\Sigma_L M$ ,  $\beta_{1 \rightarrow 2L}$ , we get

$$\sum_{i=1}^L (\beta_i - \beta_{L+i}) = \sum_{i=1}^L (\lambda_{P_i} + \lambda_{P_i}^*) = \text{tr}(\Lambda^+) - \text{tr}(\Lambda^{-t}), \quad (\text{S.30})$$

which exactly cancels the last term in the expression of  $\mathcal{L}$  in Eq.(S.15). So we can write  $\mathcal{L}$  as

$$\mathcal{L} = 2 \sum_{i=1}^L \lambda_{P_i} b'_i b_i + 2 \sum_{i=1}^L \lambda_{P_i}^* b'_{L+i} b_{L+i}. \quad (\text{S.31})$$

If there is a unique steady state, the state  $|\rho_{ss}\rangle$  which annihilates all the operator  $b'_{1 \rightarrow 2L}$  is the steady state because  $\mathcal{L}|\rho_{ss}\rangle = 0$ .

### I.B. The expectation value of $a_i^\dagger a_j$

Computing the expectation value of observable  $\hat{O}$  on the steady state, which is  $\text{tr}(\hat{O}\rho_{ss})$ , it is equivalent to the expression  $\langle \mathbf{1} | \hat{O} | \rho_{ss} \rangle$  where we have simply re-written the trace of an operator times the density matrix in the enlarged space in which the density matrix is written as a vector. In order to compute quadratic expectation values such as  $\langle \mathbf{1} | a_i^\dagger a_j | \rho_{ss} \rangle$  it is convenient to rewrite the eigenequation Eq.(S.14) in a different form.

#### I.B.1. Equation for quadratic operators

To do so we start from  $W_1^{-1} W_1 = \mathbf{1}_{2L}$  and using Eq.(S.26), we have

$$D = C - W_P^\dagger{}^{-1}; \quad (\text{S.32})$$

$$C = W_P Q, \quad (\text{S.33})$$

where  $Q$  is any Hermitian matrix. Therefore  $W_1$  can also be written as

$$W_1 = \begin{pmatrix} W_P & W_P Q \\ W_P & W_P Q - W_P^\dagger{}^{-1} \end{pmatrix} \quad (\text{S.34})$$

From the eigenequation Eq.(S.14), which can be written now as

$$\Sigma_L M W_1 = W_1 \begin{pmatrix} \lambda_P & 0 \\ 0 & -\lambda_P^* \end{pmatrix}, \quad (\text{S.35})$$

and using Eq.(S.34), and using  $X = W_P Q W_P^\dagger$  we have

$$P X + X P^\dagger = \Lambda^+. \quad (\text{S.36})$$

Solving this equation for  $X$  will prove very useful in the following.

#### I.B.2. Elements of $\text{tr}(\rho a_i^\dagger a_j)$

First, using Eqs.(S.28), we write

$$a_i^\dagger = - \sum_{k=1}^L D_{i,k}^* b'_k - \sum_{k=1}^L W_{P_{i,k}}^* b_{L+k}; \quad (\text{S.37})$$

$$a_j = \sum_{k=1}^L W_{P_{j,k}} b_k + \sum_{k=1}^L C_{j,k} b'_{L+k}. \quad (\text{S.38})$$

Using this we can write

$$a_i^\dagger a_j = - \sum_{k,l=1}^L D_{i,k}^* W_{P,j,l} b'_k b_l - \sum_{k,l=1}^L D_{i,k}^* C_{j,l} b'_k b'_{L+l} - \sum_{k,l=1}^L W_{P,i,k}^* W_{P,j,l} b_{L+k} b_l - \sum_{k,l=1}^L W_{P,i,k}^* C_{j,l} b_{L+k} b'_{L+l} \quad (\text{S.39})$$

We then show that identity bra  $\langle \mathbf{1} | = \sum_{i_1, i_2, \dots, i_L} \langle i_1, i_2, \dots, i_L, i_1, i_2, \dots, i_L |$  is annihilated by all the operators  $\mathbf{b}'_{1 \rightarrow 2L}$ . Since  $\mathbf{b}'_{1 \rightarrow L}$  and  $\mathbf{b}'_{L+1 \rightarrow 2L}$  have the same structure, we only have to prove this is the case for all  $\mathbf{b}'_{1 \rightarrow L}$ . Taking  $1 \leq i \leq L$ , and using Eq.(S.29), together with the fact that  $\langle \mathbf{1} | = \sum_{i_1, i_2, \dots, i_L} \langle i_1, i_2, \dots, i_L, i_1, i_2, \dots, i_L |$ , we have

$$\begin{aligned} \langle \mathbf{1} | b'_i &= \sum_{i_1, i_2, \dots, i_L} \langle i_1, i_2, \dots, i_L, i_1, i_2, \dots, i_L | \left( \sum_{k=1}^L W_{P,i,k}^t a_k^\dagger - \sum_{k=1}^L W_{P,i,k}^t a_{L+k} \right) \quad (\text{S.40}) \\ &= \sum_{k=1}^L W_{P,i,k}^t \left[ \sum_{i_1, i_2, \dots, i_L} \langle i_1, i_2, \dots, i_L, i_1, i_2, \dots, i_L | (a_k^\dagger - a_{L+k}) \right] \\ &= \sum_{k=1}^L W_{P,i,k}^t \sqrt{i_k} \sum_{i_1, i_2, \dots, i_L} \langle i_1, i_2, \dots, i_k - 1, \dots, i_L, i_1, i_2, \dots, i_k, \dots, i_L | \\ &\quad - \sum_{k=1}^L W_{P,i,k}^t \sqrt{i_k + 1} \sum_{i_1, i_2, \dots, i_L} \langle i_1, i_2, \dots, i_k, \dots, i_L, i_1, i_2, \dots, i_k + 1, \dots, i_L | \\ &= \sum_{k=1}^L W_{P,i,k}^t \sqrt{i_k + 1} \sum_{i_1, i_2, \dots, i_L} \langle i_1, i_2, \dots, i_k, \dots, i_L, i_1, i_2, \dots, i_k + 1, \dots, i_L | \\ &\quad - \sum_{k=1}^L W_{P,i,k}^t \sqrt{i_k + 1} \sum_{i_1, i_2, \dots, i_L} \langle i_1, i_2, \dots, i_k, \dots, i_L, i_1, i_2, \dots, i_k + 1, \dots, i_L | \\ &= 0 \end{aligned}$$

Hence, computing the trace of Eq.(S.39) we find that only the last term does not vanish and gives

$$\begin{aligned} \langle \mathbf{1} | a_i^\dagger a_j | \rho_{ss} \rangle &= - \langle \mathbf{1} | \sum_{k,l=1}^L W_{P,i,k}^* C_{j,l} b_{L+k} b'_{L+l} | \rho_{ss} \rangle = - \sum_{k,l=1}^L W_{P,i,k}^* C_{j,l} \delta_{k,l} \quad (\text{S.41}) \\ &= -(CW_P^\dagger)_{j,i} = -(W_P Q W_P^\dagger)_{j,i} = -X_{j,i} \end{aligned}$$

We define the binary observable matrix  $O_{i,j} = \text{tr}(\rho a_i^\dagger a_j)$ , then from above result we have  $O = -X^t$ .

### I.C. Important properties of the bosonic ladder

It is now useful to rewrite Eq.(S.36) in a slightly different form which is

$$hX - Xh = i(2\Lambda^+ - (\Lambda^+ - \Lambda^-)X - X(\Lambda^+ - \Lambda^-)) \quad (\text{S.42})$$

Now we consider another system whose dissipation is the same while the Hamiltonian  $h' = h^*$ . The steady state of this system, which we assume to be unique as for the original system  $h$ , will be  $X'$ .  $X'$  will then be the solution to equation

$$h^* X' - X' h^* = i(2\Lambda^+ - (\Lambda^+ - \Lambda^-)X' - X'(\Lambda^+ - \Lambda^-)) \quad (\text{S.43})$$

Taking the conjugate of both side, and writing  $X'' = X'^*$ , we get

$$hX'' - X''h = -i(2\Lambda^+ - (\Lambda^+ - \Lambda^-)X'' - X''(\Lambda^+ - \Lambda^-)) \quad (\text{S.44})$$

To show the particular properties of the ladder that we study, it is convenient to revert to a notation with two indices, one for the rung and one for the leg, i.e.  $(i,p), 1 \leq i \leq l, p = 1, 2$ , will correspond to the single index

$i + (p - 1)l$ . Therefore,  $h$  will be a four dimensional tensor, and its non-zero elements are

$$h(j, p, j + 1, p) = J_{j,p}^{\parallel}, \text{ and } h(j + 1, p, j, p) = J_{j,p}^{\parallel *}; \text{ for } 1 \leq j \leq L - 1 \quad (\text{S.45})$$

$$h(j, 1, j, 2) = J_j^{\perp}, \text{ and } h(j, 2, j, 1) = J_j^{\perp *}; \text{ for } 1 \leq j \leq L \quad (\text{S.46})$$

$$h(j, p, j, p) = \mu_{j,p} \quad (\text{S.47})$$

### I.C.1. Considering the complex conjugate of the Hamiltonian

Taking the complex conjugate of the Hamiltonian corresponds to changing the phase from  $\phi \rightarrow -\phi$ . In the following we show that in case for which the ladder potential is uniform and the dissipation is diagonal (which is the case we study),  $X''$  is related to  $X$  so that

$$X''_{j,p,j+k,p+q} = (-1)^{k+q} X_{j,p,j+k,p+q}. \quad (\text{S.48})$$

Since we assume the ladder potential to be uniform, we can effectively make it zero because any constant shift of the potential will not make any change to  $X$ . Therefore, using Eq.(S.48) in the left-hand side of Eq.(S.44) we get

$$\begin{aligned} (hX'' - X''h)_{i,m,j,n} &= \sum_{k,p} h_{i,m,k,p} X''_{k,p,j,n} - X''_{i,m,k,p} h_{k,p,j,n} \\ &= h_{i,m,i-1,m} X''_{i-1,m,j,n} + h_{i,m,i+1,m} X''_{i+1,m,j,n} + h_{i,m,i,3-m} X''_{i,3-m,j,n} \\ &\quad - X''_{i,m,j-1,n} h_{j-1,n,j,n} - X''_{i,m,j+1,n} h_{j+1,n,j,n} - X''_{i,m,j,3-n} h_{j,3-n,j,n} \\ &= (-1)^{j-i+1+n-m} h_{i,m,i-1,m} X_{i-1,m,j,n} + (-1)^{j-i-1+n-m} h_{i,m,i+1,m} X_{i+1,m,j,n} \\ &\quad + (-1)^{j-i+n+m-3} h_{i,m,i,3-m} X_{i,3-m,j,n} - (-1)^{j-i-1+n-m} * X_{i,m,j-1,n} h_{j-1,n,j,n} \\ &\quad - (-1)^{j-i+1+n-m} X_{i,m,j+1,n} h_{j+1,n,j,n} - (-1)^{j-i+3-n-m} X_{i,m,j,3-n} h_{j,3-n,j,n} \\ &= (-1)^{j-i+n-m-1} (h_{i,m,i-1,m} X_{i-1,m,j,n} + h_{i,m,i+1,m} X_{i+1,m,j,n} + h_{i,m,i,3-m} X_{i,3-m,j,n} \\ &\quad - X_{i,m,j-1,n} h_{j-1,n,j,n} - X_{i,m,j+1,n} h_{j+1,n,j,n} - X_{i,m,j,3-n} h_{j,3-n,j,n}) \\ &= (-1)^{j-i+n-m-1} (hX - Xh)_{i,m,j,n} \end{aligned} \quad (\text{S.49})$$

while its right-hand side gives

$$((\Lambda^+ - \Lambda^-)X'' + X''(\Lambda^+ - \Lambda^-))_{i,m,j,n} = (-1)^{j-i+n-m} ((\Lambda^+ - \Lambda^-)_{i,m,i,m} + (\Lambda^+ - \Lambda^-)_{j,n,j,n}) X_{i,m,j,n} \quad (\text{S.50})$$

therefore we have

$$-i(2\Lambda^+ - (\Lambda^+ - \Lambda^-)X'' - X''(\Lambda^+ - \Lambda^-))_{i,m,j,n} = (-1)^{j-i+n-m-1} i(2\Lambda^+ - (\Lambda^+ - \Lambda^-)X - X(\Lambda^+ - \Lambda^-))_{i,m,j,n} \quad (\text{S.51})$$

This proves that  $X'$  is related to  $X$  by

$$X'_{j,p,j+k,p+q} = (-1)^{k+q} X_{j,p,j+k,p+q}^* \quad (\text{S.52})$$

From this we learn that, for  $k = 1$  and  $q = 0$ ,  $X'_{j,p,j+1,p} = -X_{j,p,j+1,p}^*$ , which means the current on the legs is unchanged,  $j'_{j,p,j+1,p} = j_{j,p,j+1,p}$ . Setting  $k = 0$ ,  $p = 1$ ,  $q = 1$ , we have  $X'_{j,1,j,2} = -X_{j,1,j,2}^*$ , which means that also the current on the rungs is unchanged  $j'_{j,1,j,2} = j_{j,1,j,2}$ .

In case that the Hamiltonian is real, we know that  $X' = X$ , which means

$$X_{j,p,j+k,p+q} = (-1)^{k+q} X_{j,p,j+k,p+q}^* \quad (\text{S.53})$$

Therefore we have  $X_{j,p,j+k,p} = (-1)^k X_{j,p,j+k,p}^*$ , which means that the observables  $X_{j,p,j+2k,p}$  are purely real, and observables  $X_{j,p,j+2k+1,p}$  are purely imaginary. The observables on the rungs satisfy  $X_{j,p,j,3-p} = -X_{j,p,j,3-p}^*$ , therefore they are purely imaginary which has consequences in computing the kinetic energy on the rung which is 0.

*I.C.2. Considering a shift on the diagonals of the quadratic observable for the steady state*

Let us consider a change in  $X$  such that  $X' = X + s\mathbf{1}$ . This will give

$$hX' - X'h = hX - Xh; \quad (\text{S.54})$$

$$(\Lambda^+ - \Lambda^-)X' + X'(\Lambda^+ - \Lambda^-) = (\Lambda^+ - \Lambda^-)X + X(\Lambda^+ - \Lambda^-) + 2s(\Lambda^+ - \Lambda^-). \quad (\text{S.55})$$

Therefore,  $X'$  satisfies the equation

$$hX' - X'h = i [(2\Lambda^+ + 2s(\Lambda^+ - \Lambda^-)) - (\Lambda^+ - \Lambda^-)X' - X'(\Lambda^+ - \Lambda^-)] \quad (\text{S.56})$$

The consequences of Eq.(S.56) become apparent after rewriting, as in the main paper,  $\Lambda_{i,p}^+ = \Gamma\bar{n}_{i,p}$  and  $\Lambda_{i,p}^- = \Gamma(\bar{n}_{i,p} + \mathbf{1})$ . In fact Eq.(S.56) means that  $X'$  is a solution to another system with  $\Gamma' = \Gamma$  but with an average occupation shifted as  $\bar{n}'_{i,p} = \bar{n}_{i,p} - s$ . This is due to the fact that  $\Lambda_{i,p}^+ - \Lambda_{i,p}^- = \Gamma$  and does not depend on  $\bar{n}_{i,p}$  (here we have used the notation  $\Lambda_{i,p}^+ = \Lambda_{i,p,i,p}^+$  because the dissipator is diagonal). A change in the average occupation fixed by the dissipation thus only change the local occupations but not the currents nor the kinetic energy.

In a similar manner it is also easy to realize that  $X' = sX$  is the solution to the system with the same  $h$  and  $\Gamma$ , but  $\bar{n}' = s\bar{n}$ . A natural consequence of the results in this subsection is that, for instance, it is possible to compute the observables for the case in which one boundary is set to  $\bar{n}_{i,p} = 0$  while the other to any value and then compute all the other possible cases by a shift or a dilation in  $\bar{n}$ .

## II. Symmetries and properties of the steady state

We now explore some symmetries of the system, in case that the chemical potential is uniform.

### II.A. Case of even number of rungs

For  $l = 2N$  we can arrange the Hamiltonian so that

$$H = \{a_{1,1}, a_{3,1}, \dots, a_{2N-1,1}, a_{2,2}, a_{4,2}, \dots, a_{2N,2}\} R \{a_{1,2}^\dagger, a_{3,2}^\dagger, \dots, a_{2N-1,2}^\dagger, a_{2,1}^\dagger, a_{4,1}^\dagger, \dots, a_{2N,1}^\dagger\} + \text{H.c.} \quad (\text{S.57})$$

where the operators  $a_{i,j}$  are grouped in two different sets and the coefficient matrix  $R$  can be written as

$$R = \begin{pmatrix} A & B \\ C & D \end{pmatrix}, \quad (\text{S.58})$$

$A, B, C, D$  are  $N \times N$  matrix, which are

$$A = J^\perp \mathbf{1}_N, \quad D = J^{\perp*} \mathbf{1}_N \quad (\text{S.59})$$

$$B_{i,i} = J_{i,1}^\parallel, B_{i+1,i} = J_{i,1}^{\parallel*}; \quad (\text{S.60})$$

$$C_{i,i} = J_{i,2}^{\parallel*}, B_{i,i+1} = J_{i,2}^\parallel \quad (\text{S.61})$$

Supposing that  $R$  has the singular value decomposition  $R = USV^\dagger$ , then we can perform two unitary transformation to the system as

$$\{a_{1,1}, a_{3,1}, \dots, a_{2N-1,1}, a_{2,2}, a_{4,2}, \dots, a_{2N,2}\} = \mathbf{b}_{1 \rightarrow 2N} U; \quad (\text{S.62})$$

$$\{a_{1,2}^\dagger, a_{3,2}^\dagger, \dots, a_{2N-1,2}^\dagger, a_{2,1}^\dagger, a_{4,1}^\dagger, \dots, a_{2N,1}^\dagger\} = V^\dagger \mathbf{c}_{1 \rightarrow 2N} \quad (\text{S.63})$$

Writing  $H$  in terms of these  $4N$  new modes  $\mathbf{b}_{1 \rightarrow 2N}$ ,  $\mathbf{c}_{1 \rightarrow 2N}$ , we get

$$H = \sum_{j=1}^{2N} S_{j,j} b_j c_j^\dagger + \text{H.c.} \quad (\text{S.64})$$

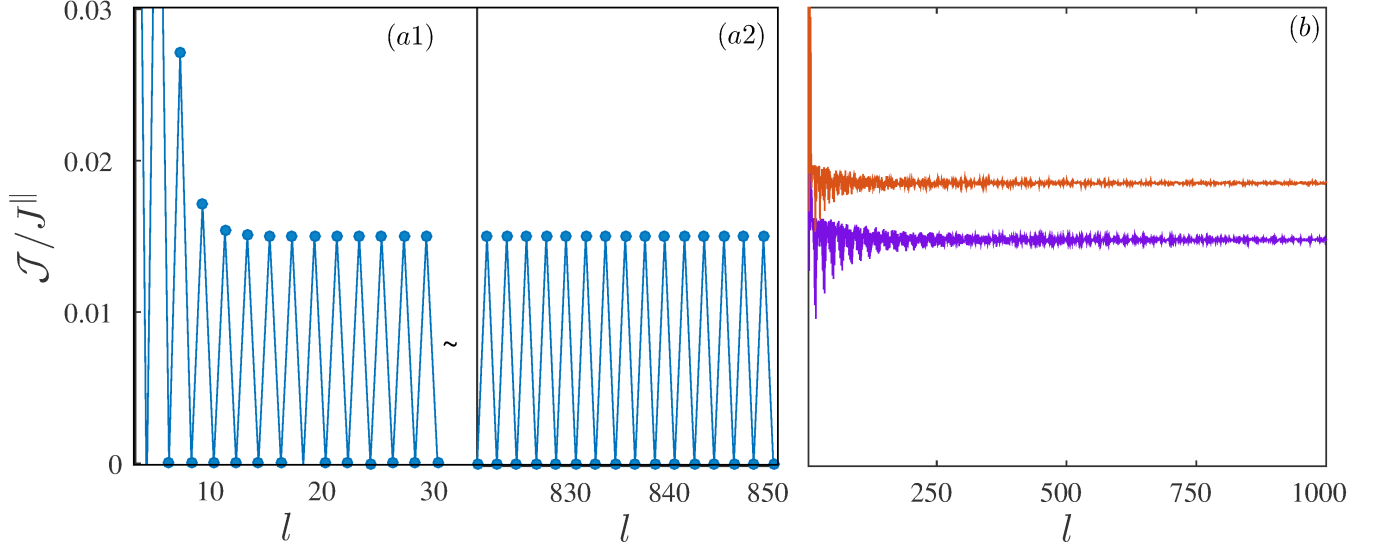


FIG. S.1: (a1-a2) Behavior of the total particle current  $\mathcal{J}$  versus the size of the ladder  $l$  when  $\phi = \pi$ . (b) Total particle current  $\mathcal{J}$  versus size of the ladder  $l$  for  $\phi/\pi = 0.9$  (yellow),  $0.95$  (purple). Here  $J^\perp = J^\parallel$ . In all the figures in the supplementary material we use  $\bar{n}_1 = 0.5$ ,  $\bar{n}_l = 0.1$  and  $\Gamma = 5J^\parallel/\hbar$ .

When  $\phi = \pi$ , i.e.  $J_{i,1}^\parallel = -J_{i,2}^\parallel$ , we have  $B = -C^\dagger$ , which results in  $R^\dagger R$  and  $RR^\dagger$  to be block diagonal. Then we can choose the left transformation  $U$  to be block diagonal

$$U = \begin{pmatrix} U_1 & 0 \\ 0 & U_2 \end{pmatrix}, \quad (\text{S.65})$$

which means

$$\{a_{1,1}, a_{3,1}, \dots, a_{2N-1,1}\} = \mathbf{b}_{1 \rightarrow N} U_1; \quad (\text{S.66})$$

$$\{a_{2,2}, a_{4,2}, \dots, a_{2N,2}\} = \mathbf{b}_{N+1 \rightarrow 2N} U_2; \quad (\text{S.67})$$

In the  $C$  configuration, the jump operator  $a_{1,1}$  of the left bath belongs to the set  $\{a_{1,1}, a_{3,1}, \dots, a_{2N-1,1}\}$ , and the jump operator  $a_{l,2}$  belongs to the set  $\{a_{2,2}, a_{4,2}, \dots, a_{2N,2}\}$ . This means that the super operator  $\mathcal{L}$  can be separated into two operator  $\mathcal{L}_1$  and  $\mathcal{L}_2$ .  $\mathcal{L}_1$  only acts on modes  $\mathbf{b}_{1 \rightarrow N}$ ,  $\mathbf{c}_{1 \rightarrow N}$ , and  $\mathcal{L}_2$  only acts on modes  $\mathbf{b}_{N+1 \rightarrow 2N}$ ,  $\mathbf{c}_{N+1 \rightarrow 2N}$ , there will be no connections between these two sub block, the first block only feels the left bath and the second block only feels the right bath. The two sub system will reach steady states independently, if there are no additional dark modes in the system. This exact symmetry for  $\phi = \pi$  and even number of rungs has an interesting consequence. In fact this implies that, even as  $L$  increases the value of the total current for even or odd number of sites ladders will have a finite distance as shown in Fig.S.1(a1-a2). As shown in Fig.2(b) instead when  $\phi \neq \pi$  the change of value between even and odd number of rungs in the ladder is finite at the beginning but it seems to converge asymptotically.

## II.B. Case of odd number of rungs

In case  $L = 2N + 1$  we can arrange the Hamiltonian so that

$$H = \{a_{1,1}, a_{3,1}, \dots, a_{2N+1,1}, a_{2,2}, a_{4,2}, \dots, a_{2N,2}\} R \{a_{1,2}^\dagger, a_{3,2}^\dagger, \dots, a_{2N+1,2}^\dagger, a_{2,1}^\dagger, a_{4,1}^\dagger, \dots, a_{2N,1}^\dagger\} + \text{H.c.}, \quad (\text{S.68})$$

where the coefficient matrix  $R$  can be written as

$$R = \begin{pmatrix} A & B \\ C & D \end{pmatrix}. \quad (\text{S.69})$$

$A$  is a matrix of dimension  $(N+1) \times (N+1)$ ,  $B$  is  $(N+1) \times N$ ,  $C$  is  $N \times (N+1)$ , and  $D$  is  $N \times N$ , which are (for  $1 \leq i \leq N$ )

$$A = J^\perp \mathbf{1}_{N+1}, D = J^\perp{}^* \mathbf{1}_N \quad (\text{S.70})$$

$$B_{i,i} = J_{i,1}^\parallel, B_{i+1,i} = J_{i,1}^\parallel{}^*; \quad (\text{S.71})$$

$$C_{i,i} = J_{i,2}^\parallel{}^*, B_{i,i+1} = J_{i,2}^\parallel \quad (\text{S.72})$$

Again when  $\phi = \pi$ , i.e.  $J_{i,1}^\parallel = -J_{i,2}^\parallel$ , we have  $B = -C^\dagger$ , and  $R^\dagger R, RR^\dagger$  are block diagonal. This means that we can find  $N+1$  by  $N+1$  matrix  $U_1$  and  $N$  by  $N$  matrix  $U_2$ , which satisfy

$$\{a_{1,1}, a_{3,1}, \dots, a_{2N+1,1}\} = \mathbf{b}_{1 \rightarrow N+1} U_1; \quad (\text{S.73})$$

$$\{a_{2,2}, a_{4,2}, \dots, a_{2N,2}\} = \mathbf{b}_{N+2 \rightarrow 2N+1} U_2 \quad (\text{S.74})$$

so that  $H$  could be written in the form equivalent to Eq.(S.64). In the  $R$  configuration, both the jump operators of the left and right bath,  $a_{1,1}$  and  $a_{2N+1,1}$ , belongs to the set  $\{a_{1,1}, a_{3,1}, \dots, a_{2N+1,1}\}$ , therefore, the super operator  $\mathcal{L}$  can be separate into two operator  $\mathcal{L}_1$  and  $\mathcal{L}_2$ .  $\mathcal{L}_1$  only acts on modes  $\mathbf{b}_{1 \rightarrow N+1}$ ,  $\mathbf{c}_{1 \rightarrow N+1}$ , and  $\mathcal{L}_2$  only acts on modes  $\mathbf{b}_{N+2 \rightarrow 2N+1}$ ,  $\mathbf{c}_{N+2 \rightarrow 2N+1}$ . Noticing that the super operator  $\mathcal{L}_2$  does not contain any bath, so that the  $2N$  modes  $\mathbf{b}_{N+2 \rightarrow 2N+1}$ ,  $\mathbf{c}_{N+2 \rightarrow 2N+1}$  will be dark modes. In the  $C$  configuration, such properties does not exist in general.

### II.C. $R$ configuration

In this section we analyse the symmetry of both the Hamiltonian and the dissipation. First, it is easy to see that if there is a unitary transformation  $U$  such that  $X' = U^\dagger X U$ , which is  $X = U X' U^\dagger$ , then  $X'$  satisfies

$$U^\dagger P U X' + X' U^\dagger P^\dagger U = U^\dagger \Lambda^+ U, \quad (\text{S.75})$$

which means that  $X'$  is the solution to the system with  $P' = U^\dagger P U$ ,  $\Lambda^{+'} = U^\dagger \Lambda^+ U$ . In the  $R$  configuration, we define the transformation  $U$  such that it is non-zero only on the anti-diagonals elements,  $U_{i,L-i+1} = 1$ , then we have

$$h' = U^\dagger h U = h^*; \quad (\text{S.76})$$

$$\Gamma' = U^\dagger \Gamma U = \Gamma \quad (\text{S.77})$$

and  $\Lambda^{+'} = U^\dagger \Lambda^+ U$  satisfies  $\Lambda^{+'}_{1,1} = \Lambda^+_{L,1}$ ,  $\Lambda^{+'}_{L,1} = \Lambda^+_{1,1}$ . From the previous discuss we know that the off diagonal terms of  $X$  is invariant if we shift  $\Lambda^+$  by a scalar. So we can just set  $\Lambda^+_{1,1} = 0$ , and this will not affect the off diagonal terms. Then we find that  $\Lambda^{+'}$  and  $\Lambda^+$  is related by

$$\Lambda^{+'} = -\Lambda^+ + \Lambda^+_{L,1} \mathbf{1}, \quad (\text{S.78})$$

This means that for the off diagonal terms we can go back to the original system by first taking the conjugate of the Hamiltonian and then reverting the dissipation. Therefore, also using Eq.(S.52),  $X'$  satisfies

$$X'_{i,p,j,q} = X_{L+1-i,p,L+1-j,q} = (-1)^{j-i+q-p+1} X_{i,p,j,q}^*, \forall (i \neq j) \vee (p \neq q) \quad (\text{S.79})$$

Let  $p = 1$ ,  $q = 2$ ,  $i = j$ , we get

$$X_{L+1-i,1,L+1-i,2} = X_{i,1,i,2}^* \quad (\text{S.80})$$

Thus we have

$$\mathcal{J}_{L+1-i,1 \rightarrow 2} = -\mathcal{J}_{i,1 \rightarrow 2} \quad (\text{S.81})$$

Therefore, in case for odd  $l = 2N+1$ , the rung current on the middle rung  $N+1$ ,  $j_{N+1-i,1,N+1-i,2} = 0$ . Let  $p = q$ ,  $j = i+1$ , we get

$$X_{L+1-i,p,L-i,p} = X_{i,p,i+1,p}^* \quad (\text{S.82})$$

Thus we have

$$\mathcal{J}_{L-i,p} = \mathcal{J}_{i,p} \quad (\text{S.83})$$

which means that the modulus of the current is symmetric under reflection symmetry around the center of the ladder.

### II.D. $C$ configuration

In this case the system Hamiltonian is invariant under the transformation  $i \rightarrow L + 1 - i$ ,  $p \rightarrow 3 - p$ , and the dissipation will be reverted, therefore we have

$$X_{L+1-i,3-p,L+1-j,3-q} = -X_{i,p,j,q}, \forall (i \neq j) \vee (p \neq q) \quad (\text{S.84})$$

Let  $i = j$ ,  $p = 1$ ,  $q = 2$ , we get

$$X_{L+1-i,2,L+1-i,1} = -X_{i,1,i,2}, \quad (\text{S.85})$$

therefore we have

$$\mathcal{J}_{L+1-i,1 \rightarrow 2} = \mathcal{J}_{i,1 \rightarrow 2} \quad (\text{S.86})$$

Let  $p = q$ ,  $j = i + 1$ , we get

$$X_{L+1-i,3-p,L-i,3-p} = -X_{i,p,i+1,p} \quad (\text{S.87})$$

Therefore we have

$$\mathcal{J}_{L-i,3-p} = \mathcal{J}_{i,p} \quad (\text{S.88})$$

This implies that the chiral current  $\mathcal{J}_c = 0$  in the  $C$  configuration.

### II.E. $S$ configuration

In this case the system has the symmetry of both the  $R$  configuration and the  $C$  configuration. This means we have

$$\mathcal{J}_{L-i,3-p} = \mathcal{J}_{i,p} = \mathcal{J}_{i,3-p}, \quad (\text{S.89})$$

which also implies that the current on the rungs  $\mathcal{J}_{i,1 \rightarrow 2}$  is 0.

## III. The bulk ladder system

Valuable insights into the transport properties are gained by studying the energy spectrum of the system. Here we reproduce results known in the literature, for example in [2], to make the work more self-contained. We consider the uniform ladder such that  $A_{j,p}^{\parallel} = A_p^{\parallel}$ ,  $A_j^{\perp} = A^{\perp}$ ,  $J_{j,p}^{\parallel} = J^{\parallel}$ ,  $J_j^{\perp} = J^{\perp}$ . We choose the local gauge as

$$A_1^{\parallel} = \phi/2; \quad (\text{S.90})$$

$$A_2^{\parallel} = -\phi/2; \quad (\text{S.91})$$

$$A_j^{\perp} = 0. \quad (\text{S.92})$$

$$(\text{S.93})$$

Because of the symmetries we need to consider only  $0 < \phi \leq \pi$ .

Doing Fourier transform of the upper and lower leg separately,

$$a_{k,p} = \frac{1}{\sqrt{l}} \sum_k e^{-ikn} a_{n,p} \quad (\text{S.94})$$

so that the kinetic terms can be written as

$$\sum_{j=1}^{l-1} (e^{i\theta} a_{j,p}^{\dagger} a_{j+1,p} + H.c.) = \sum_{k=1}^l 2 \cos(\theta + k) a_{k,p}^{\dagger} a_{k,p}; \quad (\text{S.95})$$

$$\sum_{j=1}^l (a_{j,1}^{\dagger} a_{j,2} + H.c.) = \sum_{k=1}^l (a_{k,1}^{\dagger} a_{k,2} + H.c.). \quad (\text{S.96})$$

Here  $k = 2\pi m/l$  where  $l$  is still the number of rungs and  $m$  is an integer number between  $1 - l/2$  and  $l/2$ .

Therefore, after the transformation, the Hamiltonian becomes

$$H = - \sum_k \left( 2J^{\parallel} \cos(k + \phi/2) a_{k,1}^{\dagger} a_{k,1} + 2J^{\parallel} \cos(kL - \phi/2) a_{k,2}^{\dagger} a_{k,2} + J^{\perp} a_{k,1}^{\dagger} a_{k,2} + J^{\perp} a_{k,2}^{\dagger} a_{k,1} \right). \quad (\text{S.97})$$

For  $l \rightarrow \infty$  or for periodic boundary conditions, this Hamiltonian can be diagonalized using

$$a_{k,1} = v_k \alpha_k + u_k \beta_k \quad (\text{S.98})$$

$$a_{k,2} = -u_k \alpha_k + v_k \beta_k \quad (\text{S.99})$$

and we have

$$u_k = \sqrt{\frac{1}{2} \left( 1 - \frac{\sin(k) \sin(\phi/2)}{\sqrt{(J^{\perp}/2J^{\parallel})^2 + \sin^2(k) \sin^2(\phi/2)}} \right)}; \quad (\text{S.100})$$

$$v_k = \sqrt{\frac{1}{2} \left( 1 + \frac{\sin(k) \sin(\phi/2)}{\sqrt{(J^{\perp}/2J^{\parallel})^2 + \sin^2(k) \sin^2(\phi/2)}} \right)} \quad (\text{S.101})$$

The corresponding eigenvalues are

$$E_k^{\pm} = -2J^{\parallel} \cos(k) \cos\left(\frac{\phi}{2}\right) \pm \sqrt{4J^{\parallel 2} \sin^2(k) \sin^2\left(\frac{\phi}{2}\right) + J^{\perp 2}} \quad (\text{S.102})$$

### III.A. Quantum phase transition

Studying the lower energy band we can study the quantum phase transition

$$E_k^- = -2J^{\parallel} \left( \cos(k) \cos\left(\frac{\phi}{2}\right) + \sqrt{\sin^2(k) \sin^2\left(\frac{\phi}{2}\right) + t^2} \right), \quad (\text{S.103})$$

where we have used  $t = J^{\perp}/2J^{\parallel}$ . The minimum of the potential is given by  $dE_k^-/dk = 0$ , which gives

$$dE_k^-/dk = 2J^{\parallel} \left( \sin(k) \cos\left(\frac{\phi}{2}\right) - \frac{\sin(k) \cos(k) \sin^2(\phi/2)}{\sqrt{\sin^2(k) \sin^2(\phi/2) + t^2}} \right) = 0, \quad (\text{S.104})$$

$k_1 = 0$ ,  $k_2 = \pi$  are obviously solutions of the above equation, the other solutions satisfy

$$\cos(k_3) = \cot\left(\frac{\phi}{2}\right) \sqrt{\sin^2\left(\frac{\phi}{2}\right) + t^2}; \quad (\text{S.105})$$

$$k_3 = \pm \arccos\left(\cot\left(\frac{\phi}{2}\right) \sqrt{\sin^2\left(\frac{\phi}{2}\right) + t^2}\right), \quad (\text{S.106})$$

The minimum occurs either at  $k = 0$  or at  $k = \pm k_3$  and the transition occurs for a critical phase  $\phi_c$

$$\phi_c = 2 \arccos\left(\frac{\sqrt{t^2 + 4} - t}{2}\right), \quad (\text{S.107})$$

### III.B. Gap opening

When the gap opens, as shown in the main paper, the current drops and the current distribution may be altered. The gap opens when the maximum of the lower band has the same energy as the minimum of the highest band. This can be easily computed as it happens for  $E_0^+ = E_\pi^-$  which gives  $\cos(k) \leq 1 - t/\cos(\phi/2)$  and can have solutions for  $J^\perp < 2J^\parallel$ . The overlap of the two bands starts when the higher band is at its minimum, which happens at  $k = 0$  where

$$E_{k=0}^+ = -2J^\parallel \left[ \cos\left(\frac{\phi}{2}\right) - t \right] \quad (\text{S.108})$$

Next we solve  $E_k^- = E_{k=0}^+$ , which is

$$\cos^2(k) + 2\cos(\phi/2)(t - \cos(\phi/2))\cos(k) + 2\cos^2(\phi/2) - 2t\cos(\phi/2) - 1 = 0, \quad (\text{S.109})$$

the solution of which is

$$k = \pm \arccos\left(2\cos\left(\frac{\phi}{2}\right)\left(\cos\left(\frac{\phi}{2}\right) - t\right) - 1\right). \quad (\text{S.110})$$

The lower band change from single minimum to double minimum when  $\phi \leq \phi_c$ , and at the same time the upper band change from single maximum to double maximum. When this happens, the energy in the lower band becomes degenerate with period  $k = 2k_3$ , while the energy in the upper band becomes degenerate with period  $k = 2\pi - 2k_3$ .

### IV. Bulk for $\phi = 0$ and $\pi$ and geometrical coupling of the bath

When there is no gauge field it is possible to do a transformation which turns the ladder system in two independent chains. Choosing in fact  $c_{j,1} = (\hat{a}_{j,1} + \hat{a}_{j,2})/\sqrt{2}$  and  $c_{j,2} = (\hat{a}_{j,1} - \hat{a}_{j,2})/\sqrt{2}$  the Hamiltonian describing the system becomes

$$\hat{H} = -J^\parallel \left( \sum_{j=1}^{l-1} c_{j,1}^\dagger c_{j+1,1} + c_{j,2}^\dagger c_{j+1,2} + \text{H.c} \right) + 2J^\perp \sum_{j=1}^l (c_{j,2}^\dagger c_{j,2} - c_{j,1}^\dagger c_{j,1}) \quad (\text{S.111})$$

which is the Hamiltonian for two non-interacting chains, one of which has a local potential which is  $J^\perp$  higher than the other.

It is the coupling with the dissipator that may couple the chains. In fact rewriting the dissipator in term of  $c_{j,p}$  gives

$$\begin{aligned} \frac{\mathcal{D}(\hat{O})}{\Gamma} = & \sum_j \left\{ \langle \hat{n}_j \rangle \left[ 2(c_{j,1} \hat{O} c_{j,1}^\dagger + c_{j,2} \hat{O} c_{j,2}^\dagger) - (c_{j,1} c_{j,1}^\dagger + c_{j,2} c_{j,2}^\dagger) \hat{O} - \hat{O} (c_{j,1} c_{j,1}^\dagger + c_{j,2} c_{j,2}^\dagger) \right] \right. \\ & + \nu_j \langle \hat{n}_j \rangle \left[ 2(c_{j,1} \hat{O} c_{j,2}^\dagger + c_{j,2} \hat{O} c_{j,1}^\dagger) - (c_{j,2} c_{j,1}^\dagger + c_{j,1} c_{j,2}^\dagger) \hat{O} - \hat{O} (c_{j,2} c_{j,1}^\dagger + c_{j,1} c_{j,2}^\dagger) \right] \\ & + (\langle \hat{n}_j \rangle + 1) \left[ 2(c_{j,1}^\dagger \hat{O} c_{j,1} + c_{j,2}^\dagger \hat{O} c_{j,2}) - (c_{j,1}^\dagger c_{j,1} + c_{j,2}^\dagger c_{j,2}) \hat{O} - \hat{O} (c_{j,1}^\dagger c_{j,1} + c_{j,2}^\dagger c_{j,2}) \right] \\ & \left. + \nu_j (\langle \hat{n}_j \rangle + 1) \left[ 2(c_{j,1}^\dagger \hat{O} c_{j,2} + c_{j,2}^\dagger \hat{O} c_{j,1}) - (c_{j,2}^\dagger c_{j,1} + c_{j,1}^\dagger c_{j,2}) \hat{O} - \hat{O} (c_{j,2}^\dagger c_{j,1} + c_{j,1}^\dagger c_{j,2}) \right] \right\}. \quad (\text{S.112}) \end{aligned}$$

It is thus obvious that when  $\Delta_j = 0$  the chains stay decoupled even in presence of a bath. However for any finite  $\Delta_j$  the chains will be coupled. Note that depending on the geometrical coupling to the baths (i.e. depending on the relationship between  $\Delta_1$  and  $\Delta_L$ ), the ladder may have twisted boundary conditions analogous to [3].

Similarly to the case  $\phi = 0$ , when the gauge field has value  $\phi = \pi$  it is possible to do a transformation which turns the ladder systems in two independent chains. Choosing again  $d_{j,1} = (\hat{a}_{j,1} - (-1)^j \hat{a}_{j,2})/\sqrt{2}$  and  $d_{j,2} = (\hat{a}_{j,1} + (-1)^j \hat{a}_{j,2})/\sqrt{2}$  the Hamiltonian describing the system becomes

$$\hat{H} = -J^\parallel \left( \sum_{j=1}^{l-1} d_{j,1}^\dagger d_{j+1,1} + d_{j,2}^\dagger d_{j+1,2} + \text{H.c} \right) + 2J^\perp \sum_{j=1}^l (-1)^j (d_{j,2}^\dagger d_{j,2} - d_{j,1}^\dagger d_{j,1}) \quad (\text{S.113})$$

which is the Hamiltonian for two non-interacting chains in which the local potential alternates at every site.

### V. Chiral current as the system size increases

Phase transitions show a sharp behavior in the thermodynamic limit. Here we show how the chiral current changes when varying the length of the ladder  $l$ . In Fig.S.2 it is shown how, as  $l$  increases from 50 to 500, the transition becomes sharper and the oscillations are strongly reduced in magnitude. In Fig.S.3 we also show that for the particular case of  $\phi = 0$  the chiral current tends to 0 only in the limit of large  $l$  while, for finite sizes, it may have a finite value.

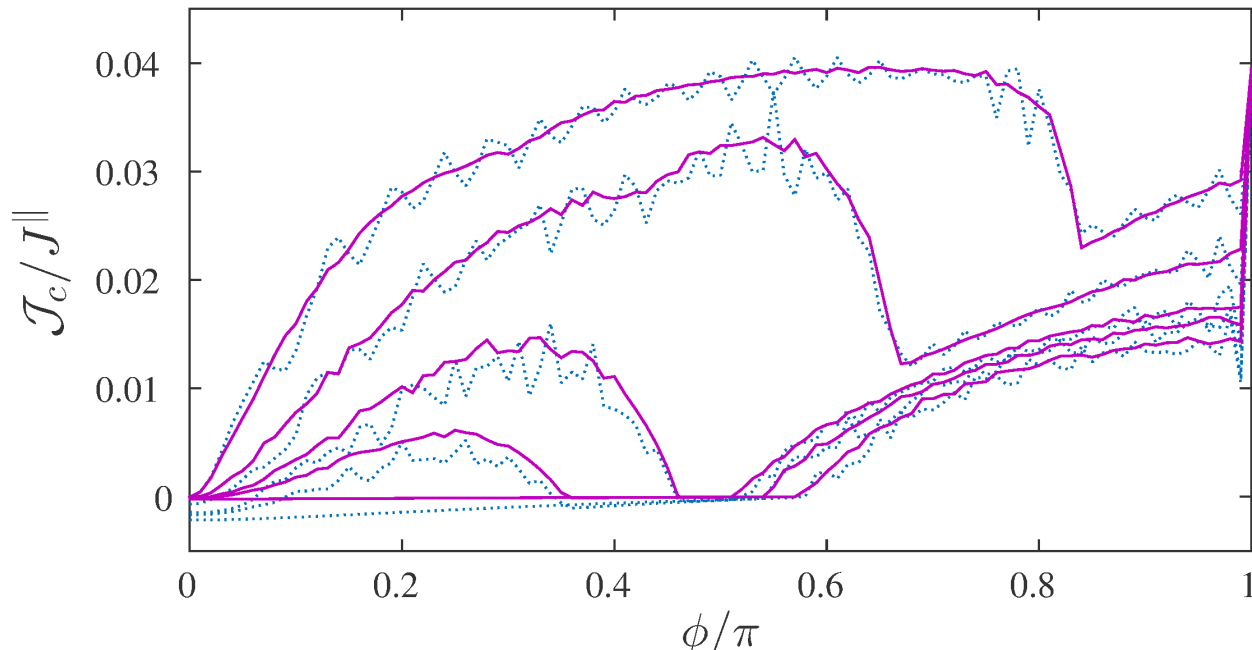


FIG. S.2: Chiral current  $\mathcal{J}_c$  versus phase  $\phi$  for  $J^\perp/J^\parallel = 0.5, 1, 1.5, 1.7, 2$  in the  $R$  configuration. The continuous purple line is the results for a length  $l = 500$  while the dotted blue line for  $l = 50$ .

### VI. Total current as a function of dissipation strength $\Gamma$

The transition occurs when the coupling within the bands is strong enough and the geometry allows it. In Fig.S.4 we show the total current  $\mathcal{J}$  versus  $\phi$  for different values of  $\Gamma$ . We see in Fig.S.4(a) that in the symmetric configuration  $S$  the transition does not occur even for  $\Gamma$  as large as  $20J^\parallel$ . Instead for the reflection symmetric configuration  $R$  as  $\Gamma$  increases a sharp transition emerges, see Fig.S.4(b).

### VII. Total current as a function of length $l$ of the ladder

For ballistic systems the total current is independent on the system size and in this model, independent on the parameters chosen, for large  $l$  the current is approximately constant as shown in Fig.S.5.

- 
- [1] T. Prosen, *New J. Phys.* **10**, 043026 (2008).
  - [2] A. Tokuno, A. Georges, *New J. Phys.* **16**, 073005 (2014).
  - [3] D. Karevski, V. Popkov, G.M. Schutz, *Phys. Rev. Lett.* **110**, 047201 (2013).
  - [4] D. Manzano, J. Cao, arXiv:1507.05705 (2015).
-

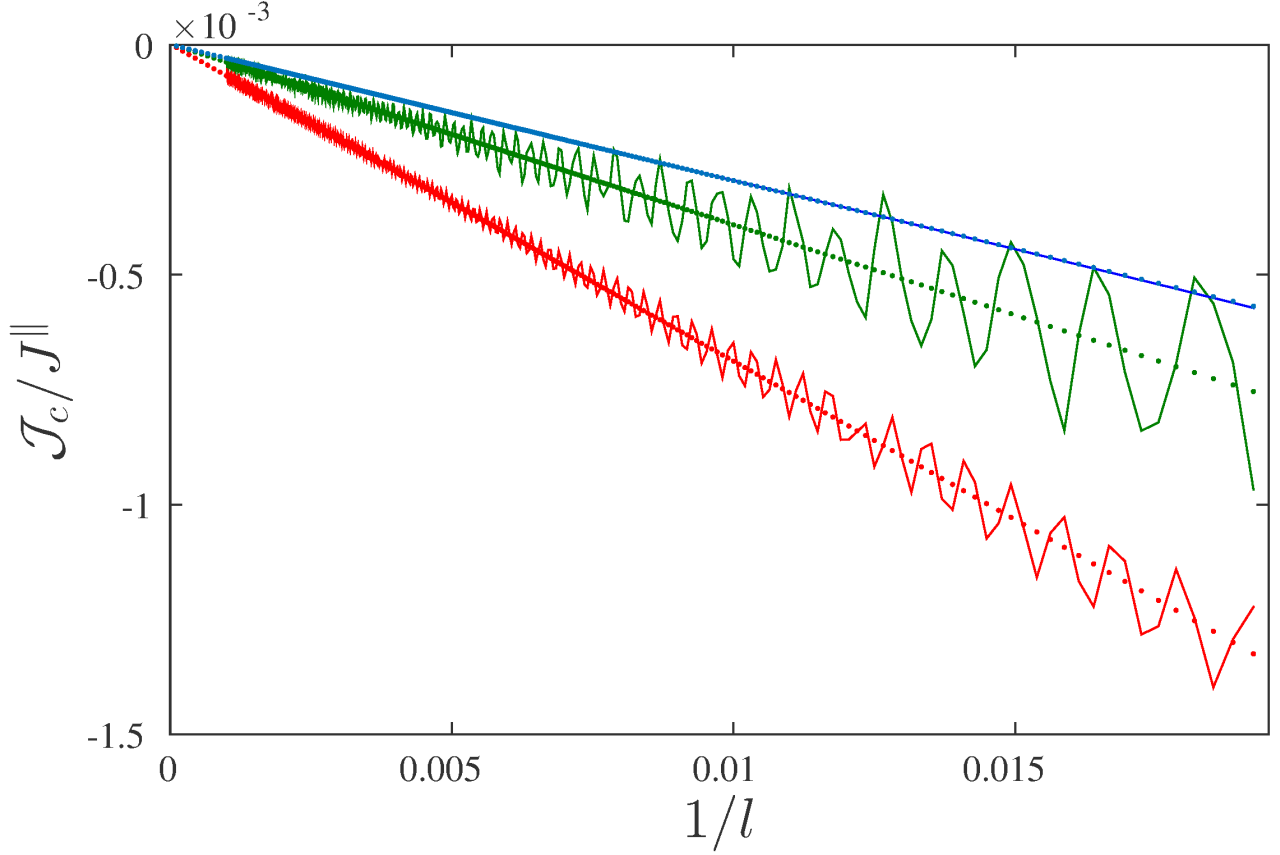


FIG. S.3: Chiral current  $\mathcal{J}_c$  versus inverse length of the chain  $1/l$  in the  $R$  configuration for  $\phi = 0$  and for  $J^\perp/J^\parallel = 3, 1, 1.5$  from top to bottom. The dotted lines are linear fits to the data.

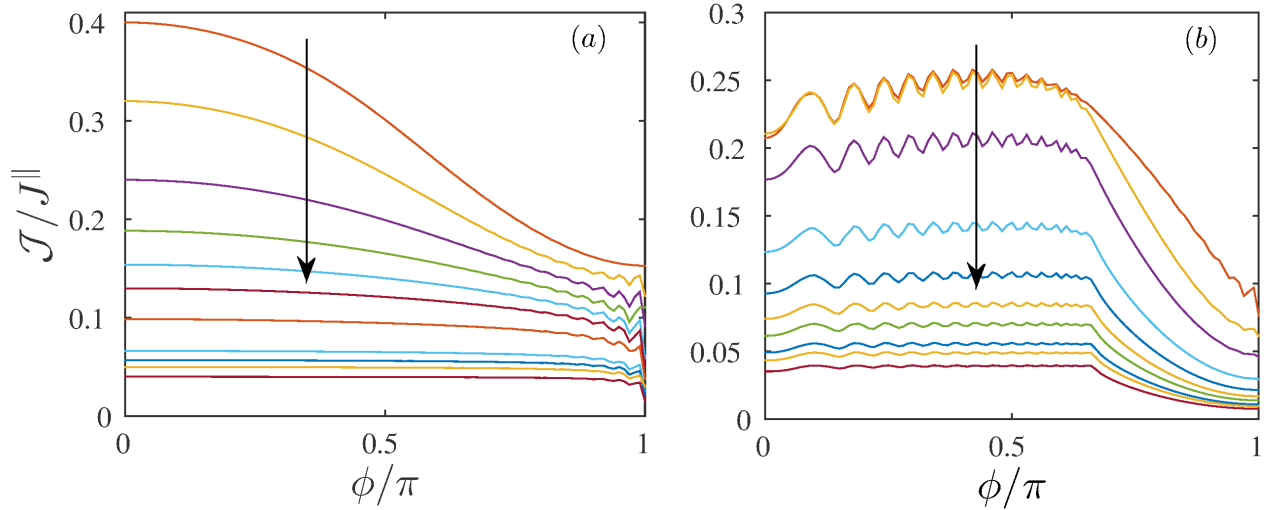


FIG. S.4: Total current  $\mathcal{J}$  versus gauge field intensity  $\phi$  for different value of dissipation strength  $\Gamma$  in the symmetric configuration  $S$  (a) and in the reflection symmetric configuration  $R$  (b). The values of  $\hbar\Gamma/J^\parallel$  increase in the direction of the arrow and are 1, 2, 3, 4, 5, 6, 8, 12, 14, 16, 20 in (a) and 1, 2, 3, 5, 7, 9, 11, 14, 16, 20 in (b). In both figures  $J^\perp = J^\parallel$  and the length is  $l = 200$ .

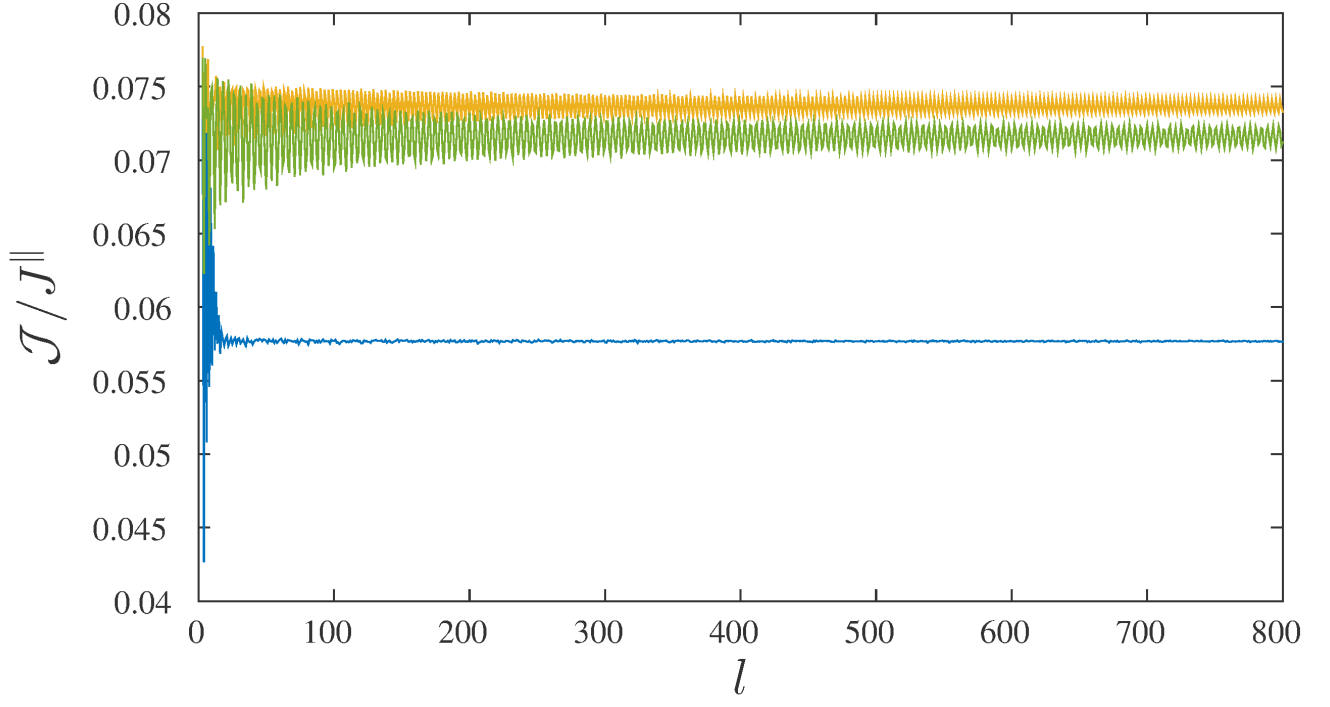


FIG. S.5: Total current  $\mathcal{J}$  versus ladder length  $l$  for  $J^{\perp} = J^{\parallel}$  and  $\phi$  equal to, from top to bottom,  $\pi/2$ ,  $0.3\pi$  and  $0.7\pi$ .